Rap1b facilitates NK cell functions via IQGAP1-mediated signalosomes

Aradhana Awasthi,[1] Asanga Samarakoon,[1] Haiyan Chu,[1] Rajasekaran Kamalakannan,[1] Lawrence A. Quilliam,[5] Magdalena Chrzanowska-Wodnicka,[3] Gilbert C. White II,[2] and Subramaniam Malarkannan[1,4]

[1]Molecular Immunology, [2]Platelet, and [3]Vascular Signaling, Blood Research Institute, [4]Department of Medicine, Medical College of Wisconsin, Milwaukee, WI 53226
[5]Department of Biochemistry and Molecular Biology, Indiana University School of Medicine, Indianapolis, IN 46202

The Journal of Experimental Medicine

Rap1 GTPases control immune synapse formation and signaling in lymphocytes. However, the precise molecular mechanism by which Rap1 regulates natural killer (NK) cell activation is not known. Using Rap1a or Rap1b knockout mice, we identify Rap1b as the major isoform in NK cells. Its absence significantly impaired LFA1 polarization, spreading, and microtubule organizing center (MTOC) formation in NK cells. Neither Rap1 isoform was essential for NK cytotoxicity. However, absence of Rap1b impaired NKG2D, Ly49D, and NCR1-mediated cytokine and chemokine production. Upon activation, Rap1b colocalized with the scaffolding protein IQGAP1. This interaction facilitated sequential phosphorylation of B-Raf, C-Raf, and ERK1/2 and helped IQGAP1 to form a large signalosome in the perinuclear region. These results reveal a previously unrecognized role for Rap1b in NK cell signaling and effector functions.

CORRESPONDENCE
Subramaniam Malarkannan:
subra.malar@bcw.edu

Abbreviations used: BMDC, BM-derived dendritic cell; Con A, concanavalin A; GAP, GTPase-activating protein; GTP, Guanosine 5′-triphosphate; IQGAP1, IQ domain-containing GTPase-activating-like protein; LFA1, lymphocyte function-associated antigen 1; MTOC, microtubule organizing center; MZ, marginal zone; NCR1, NK cell receptor 1; NKG2D, NKG2 type II membrane protein D; Rap1, Ras-associated protein 1; SMAC, supramolecular activation cluster.

The Ras-mediated Raf–MEK–ERK activation pathway controls many fundamental cellular processes. Rap1 belongs to the Ras superfamily, and their role in regulating NK cell development and functions is not understood. Rap1a and Rap1b isoforms are able to regulate cell proliferation, differentiation, adhesion, and polarization (Stork and Dillon, 2005). These two share >95% amino acid homology (Rousseau-Merck et al., 1990). Conversion of inactive Rap1-GDP to active Rap1-GTP is regulated by multiple guanine nucleotide exchange factors such as C3G, RasGRP/CalDAG-GEFs, and EPACs (Gotoh et al., 1995; de Rooij et al., 1998; Kawasaki et al., 1998). Rap1 signaling is terminated by GTPase-activating proteins (GAPs) such as SPA-1 and RapGAPs (Rubinfeld et al., 1991; Kurachi et al., 1997).

Rap1 regulates diverse downstream effectors including B-Raf and C-Raf, whose phosphorylation depends on active Rap1-GTPase and play a critical role in the sequential activation of MEK1/2 and their substrates ERK1/2 (Jin et al., 2006; Romano et al., 2006). Recent studies have shown that scaffolding proteins such as IQGAP (1, 2, and 3), KSR1, MP1, or Paxillin can function as signal processing centers by bringing together GTPases, kinases, and their substrates (Sacks, 2006). IQGAP1 can bind to both Rap1a and Rap1b (Jeong et al., 2007). IQGAP1 is widely expressed in multiple tissues including lymphocytes. The N-terminal calponin homology domain of IQGAP1 binds to actin and the IQ domain recruits calmodulin (Joyal et al., 1997). The C-terminal end of IQGAP1 engages with Cdc42-GTP (Joyal et al., 1997), Rac1-GTP (Hart et al., 1996), E-cadherin (Kuroda et al., 1998), β-catenin (Li et al., 1999), and APC (Watanabe et al., 2004). IQGAP1 also has the ability to bind to B-Raf (Ren et al., 2007), MEK1/2 (Roy et al., 2005), and ERK1/2 (Roy et al., 2004). Irrespective of these findings, IQGAP1-mediated signalosome formation and its relevance in regulating lymphocyte functions have not been investigated.

Recently, we generated *Rap1a* and *Rap1b* gene knockout mice (Chrzanowska-Wodnicka

The Rockefeller University Press $30.00
J. Exp. Med.
www.jem.org/cgi/doi/10.1084/jem.20100040

et al., 2005; Li et al., 2007). Here, we found that the lack of Rap1a or Rap1b did not alter the development or cytotoxicity of NK cells. However, LFA1 polarization, cell spreading of NK cells, and their ability to home and traffic were significantly reduced in the absence of Rap1b. Lack of Rap1b, but not Rap1a, resulted in severe impairment of NKG2D, Ly49D, and NCR1-mediated cytokine and chemokine generation. Upon activation, Rap1b associated with B-Raf or C-Raf and colocalized with IQGAP1 complex. The absence of Rap1b reduced B-Raf, C-Raf, and ERK1/2 phosphorylation in NK cells. Rap1b helped IQGAP1 to form a large signalosome in the perinuclear region to coordinate the phosphorylation of ERK1/2. Rap1b also colocalized with the MTOC and regulated its size and proper formation. These results reveal a previously unrecognized role of Rap1 in signalosome formation and regulation of effector functions in lymphocytes.

RESULTS

Rap1b is the major isoform in NK cells

Two highly homologous isoforms of Rap1 exists in lymphocytes. To determine the differential expression of these isoforms in NK cells, we used Rap1a$^{-/-}$ and Rap1b$^{-/-}$ mice. These mice were maintained by Het × Het breeding. The wild-type controls *Rap1a*$^{+/+}$ and *Rap1b*$^{+/+}$ that express both the isoforms were used throughout this study. First, we quantified the expression of total Rap1 proteins using an antibody that recognizes both the isoforms. Abundant amounts of Rap1 protein were present in IL-2–cultured splenic NK cells (Fig. 1 A). However, only a residual level of Rap1 protein was present in NK cells from *Rap1b*$^{-/-}$ mice. This was not caused by a differential affinity because anti-Rap1 antibody detected both recombinant Rap1a and Rap1b with similar affinities (Fig. 1 B). Based on these, we conclude that the residual protein band in *Rap1b*$^{-/-}$ NK cells represents Rap1a. We also quantified the independent levels of Rap1a and Rap1b proteins using isoform-specific mAbs. No compensatory expressions of Rap1a in NK cells from *Rap1b*$^{-/-}$ mice were found. Rap family has additional members such as Rap2 (a, b, and c; Rousseau-Merck et al., 1990). Analyses of Rap2 isoforms encoding mRNA indicated that none of the Rap2 isoforms were up-regulated in the absence of Rap1a or Rap1b in these mice (unpublished data). Confocal analyses indicated that Rap1 and Rap2 were present throughout the cytoplasm of NK cells (Fig. S1 A). Rap1 was present in membrane ruffles, cytoplasm and in the perinuclear regions. Although, Rap2 followed similar patterns, its localization was largely nonoverlapping to Rap1. Because Rap1 displayed a vesicular structure, we also co-stained NK cells with the lysosomal dye lysotracker. Results presented in Fig. S1 B demonstrate Rap1 is localized to a distinct compartment different from that of lysosomes. Collectively, these observations indicate that the Rap1b is the major isoform in NK cells and none of the other Rap family members compensated for the lack of Rap1b.

To investigate the role of Rap1 isoforms in lymphocyte development, we performed phenotypic characterization of T, B, and NK cells. The cellularity of spleen, BM thymus, mesenteric LN, lung, and liver from knockout mice were comparable to that of wild-type mice (unpublished data). Comparable percent and absolute numbers of T (CD3^{+}NK1.1^{-}) and NK (CD3^{-}NK1.1^{+}) cells were present in all the mice (Fig. S1 C). Expression of CD122, CD43, NK1.1, NKG2D, NCR1, KLRG1, CD11a, CD11b, CD49b, and CD51 were intact in *Rap1a*$^{-/-}$ and *Rap1b*$^{-/-}$ mice (Fig. S2 A). Acquisition of CD27 and Ly49 by immature NK cells that is critical to generate the NK 'repertoire' proceeded normally in the absence of Rap1 isoforms (Fig. S2, B and C). T cell development appeared to be normal in thymus and spleen based on CD4^{+} and CD8^{+} or CD4^{+}CD8^{+} staining patterns (Fig. S3, A and B). Percentages of CD19^{+} or B220^{+} B cells were comparable between different mice in the BM and spleen (Fig. S3, C and D). Lack of Rap1a or Rap1b did not affect the percentages of immature (IgM^{+}IgD$^{Low/-}$) or mature (IgM^{+}IgD^{+} or IgM^{-}IgD^{+}) B cell populations in the BM and spleen. The percentages of splenic follicular B (CD21$^{Low/-}$CD23^{Hi}) cells were comparable. However, the marginal zone (MZ) B (CD21^{Hi}CD23$^{Low/-}$) cells in *Rap1b*$^{-/-}$ mice were significantly reduced, whereas the newly forming (CD21$^{Low/-}$CD23$^{Low/-}$) cells were relatively increased. MZ B cells can also be defined by their exclusive high level expression of IgM, CD21, and CD1^{d}. Staining for these markers confirmed the reduction in IgM^{High}CD21^{High} and IgM^{High}CD1d^{High} B cell population in both *Rap1a*$^{-/-}$ and *Rap1b*$^{-/-}$ mice (Fig. S3 E). These results indicate Rap1-GTPases play critical roles in B (Chu et al., 2008) but not in NK or T cell development.

Rap1b regulates LFA1 polarization and NK spreading

Integrins are the critical components of lymphocyte trafficking, homing and successful synapse formation between the effector and the target cells. To investigate the role of Rap1 in NK cell functions, we analyzed the LFA1 polarization. NK cells were stimulated with PMA and ionomycin and stained for LFA1 and F-actin. Our results show that the *Rap1a*$^{+/+}$ or *Rap1b*$^{+/+}$ NK cells were able to polarize LFA1 in a focal point on the cell surface. However, the absence of Rap1a or Rap1b significantly impaired mobilization and clustering of LFA1 on the cell surface. NK cells from the *Rap1a*$^{-/-}$ mice formed multiple incomplete LFA1 clusters, and a vast quantity of LFA1 failed to travel to the cell surface (Fig. 1, C and D). This defect was not observed in *Rap1b*$^{-/-}$ NK cells, which could transport the LFA1 to the cell surface but failed to polarize. Both Rap1a and Rap1b isoforms have been implicated in cell spreading (Lin et al., 2008). To assess the exclusive contribution of Rap1a and Rap1b, we tested the ability of IL-2–cultured NK cells to spread on anti-LFA1 mAb or recombinant ICAM1-Fc–coated culture plates. Results presented in Fig. 1 (E and F) indicate that Rap1b, but not Rap1a, is critical for LFA1-mediated NK cell spreading. Thus, although Rap1a$^{-/-}$ NK cells formed an incomplete LFA1 cluster, the presence of Rap1b was sufficient for cells to spread onto the anti-LFA1–coated plates. None of the NK cells efficiently spread on anti-NKG2D or control isotype mAb-coated plates, demonstrating

their specificity. We conclude that among the two isoforms, Rap1b critically contributes toward the LFA1 polarization and LFA1-mediated NK cell spreading.

Rap1b regulates NK cell homing and trafficking

To address the possible defects in the trafficking of NK cells, we first analyzed the cellular organization of splenic follicular structures. The injection of the mitogen concanavalin A (Con A) has been shown to induce the redistribution of NK cells inside the spleen. In the nonchallenged mice, lack of Rap1a or Rap1b did not alter the distribution of NK cells inside the red pulp areas (Fig. 2, A–D). However, the organization of metallophilic macrophages around the follicles were drastically altered and reduced in *Rap1b*$^{-/-}$ mice (Fig. 2 D). After treatment with Con A, *Rap1b*$^{+/+}$ NK cells progressively moved into and colonized the white pulp area (Fig. 2 E); however, *Rap1b*$^{-/-}$ NK cells remained in the red pulp and failed to traffic inside the follicles (Fig. 2, F and G). To determine the role of Rap1b in regulating NK cell homing, we conducted transplant experiments. Splenocytes from *Rap1b*$^{-/-}$ and *Rap1b*$^{+/+}$ were individually labeled with TAMRA and CFSE, respectively, premixed, and intravenously injected into *Rap1b*$^{+/+}$

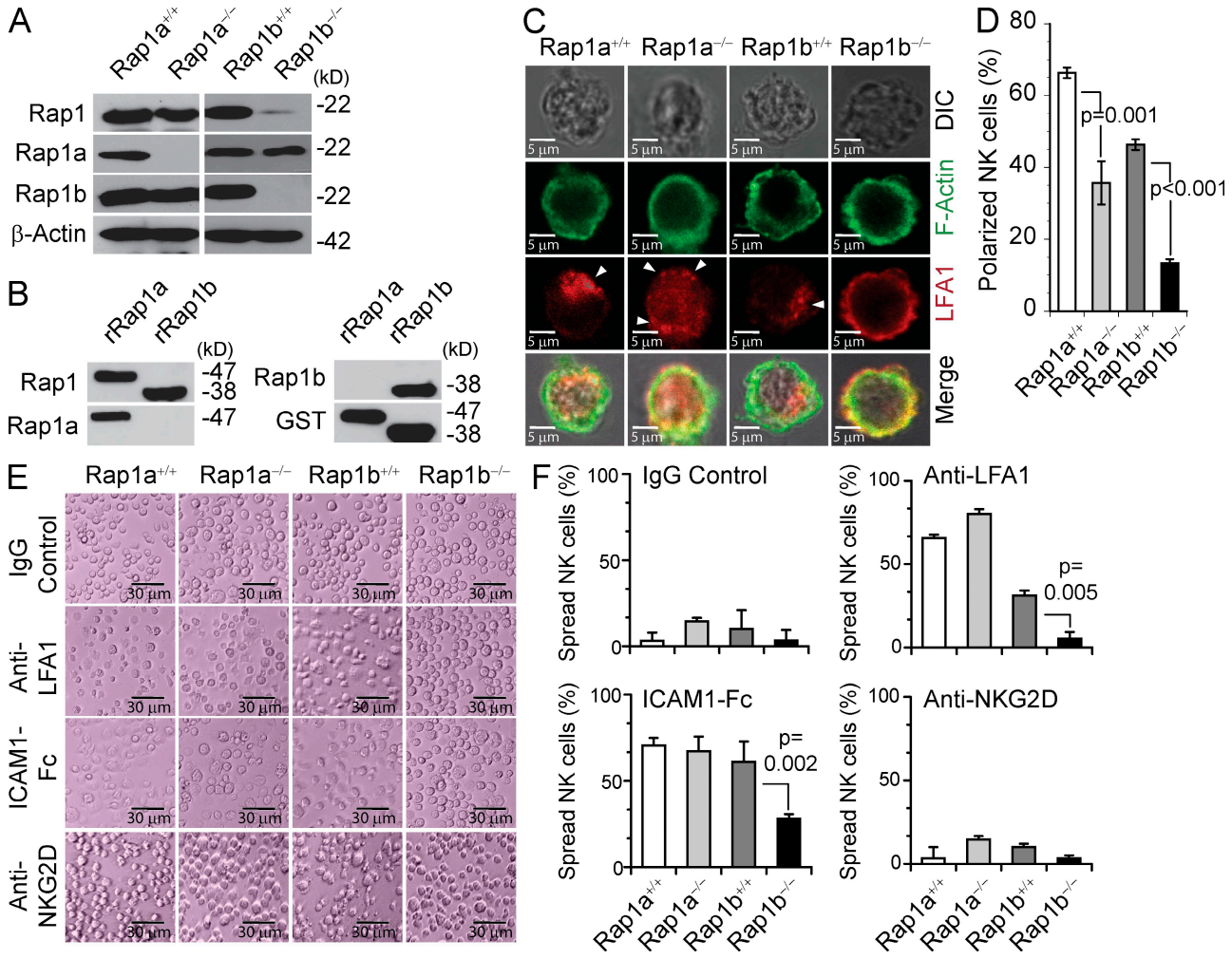

Figure 1. Rap1b is the major isoform, and its absence affects LFA1 polarization and NK cell spreading. (A) Expression levels of total Rap1, Rap1a, or Rap1b were analyzed in IL-2–cultured splenic NK cells from the indicated mice. (B) Western blot of recombinant GST-Rap1a (full-length Rap1a) and GST-Rap1b (85-184aa Rap1b) with anti-total Rap1, anti-Rap1a, anti-Rap1b, and anti-GST antibodies. (C and D) IL-2–cultured splenic NK cells were activated with PMA and ionomycin and stained for F-actin (green) and LFA1 (red). Images representative of individual or merged confocal images are shown (C). A total of 225 (*Rap1a*$^{+/+}$), 219 (*Rap1a*$^{-/-}$), 184 (*Rap1b*$^{+/+}$), and 199 (*Rap1b*$^{-/-}$) NK cells were analyzed. Localization of LFA1 in a focal point that is less than one fourth of the cell's total diameter was taken as successful polarization. Arrowheads mark the polarized LFA1. Percentages of polarized cells are shown in D. (E and F) ELISA plates were coated with isotype control (IgG), anti-LFA1 (M17/4), anti-NKG2D (A10; each 5 μg/ml), or recombinant ICAM1-Fc (5 μg/ml) and used to stimulate NK cells. Phase-contrast images were obtained after 3 h of incubation, and the spread cells were defined as the ones that lacked clearly visible edges (E). Bar graphs represent the percentages of spread NK cells. The following numbers of NK cells were analyzed for isotype control, anti-NKG2D, ICAM1-Fc, and anti-LFA1, respectively for indicated genotypes: *Rap1a*$^{+/+}$, 464, 356, 396, and 260; *Rap1a*$^{-/-}$, 404, 299, 372, and 286; *Rap1b*$^{+/+}$, 417, 260, 319, and 265; and *Rap1b*$^{-/-}$, 403, 487, 411, and 517. (F). Results presented in A-F were representatives of a minimum of three independent experiments.

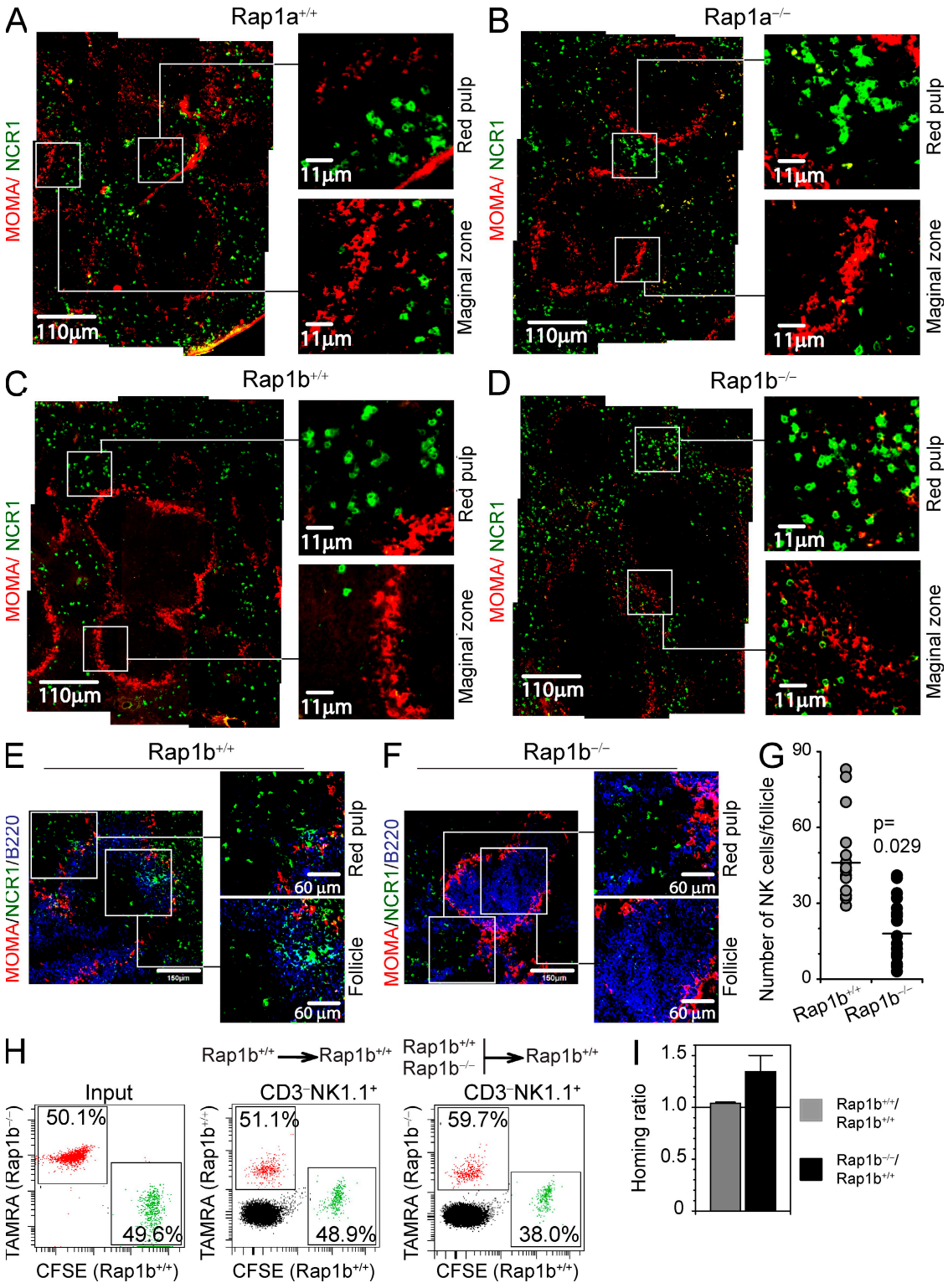

Figure 2. In vivo trafficking and homing of NK cells. (A–D) Spleen cryosections (7 µm thick) from *Rap1a*$^{+/+}$ (A), *Rap1a*$^{-/-}$ (B), *Rap1b*$^{+/+}$ (C), and *Rap1b*$^{-/-}$ (D) mice were stained with anti-MOMA (red) or anti-NCR1 (green) and analyzed in immunofluorescence microscope. Data shown are 12 individual 20× images assembled into a single panel for each genotype. White boxes indicate a select area that is enlarged to show details. Top enlarged images for each genotype represents NK cells (green) in the red pulp area. Bottom enlarged images show organization of metallophilic macrophages (red) around each follicle. A minimum of 40 white pulp areas were analyzed for each genotype. Images represent data analyzed from seven mice for each genotype. Bars: (assembled) 110 µm; (enlarged) 11 µm. Data shown are one representative set out of. (E–G) Spleens from *Rap1b*$^{+/+}$ (E) or *Rap1b*$^{-/-}$ (F)

mice. After 3 h, cells from the recipient spleen were stained with anti-NK1.1 and -CD3ε mAbs, and the ratio of *Rap1b*$^{-/-}$ to *Rap1b*$^{+/+}$ mouse-derived lymphocytes were quantified (Fig. 2, H and I). The ability of *Rap1b*$^{-/-}$ NK cells to migrate and home into the spleen was not affected; however, the proportion of *Rap1b*$^{-/-}$ NK cells that remained in the recipient spleen after 3 h were significantly higher (~40–50%) compared with that of *Rap1b*$^{+/+}$ NK cells. Together, we conclude that Rap1b plays a critical role in the in vivo homing and trafficking of NK cells.

Activation via NKG2D converts Rap1-GDP to Rap1-GTP

NKG2D is a major activation receptor of NK cells. To determine whether Rap1 isoforms are activated downstream of NKG2D, we stimulated IL-2–cultured splenic NK cells and quantified the active Rap1-GTP by a pull-down assay using GST-coupled RalGDS-RBD. NKG2D-mediated activation of *Rap1a*$^{+/+}$ or *Rap1b*$^{+/+}$ NK cells led to an increase in the quantity of active Rap1-GTP. In *Rap1a*$^{-/-}$ NK cells, where Rap1b was the only isoform present, a considerable level of active Rap1-GTP or Rap1b-GTP could be seen after activation. In contrast, NKG2D-mediated activation of *Rap1b*$^{-/-}$ NK cells resulted in reduced levels of Rap1-GTP or Rap1b-GTP (Fig. 3 A). These results indicate that Rap1b can be activated downstream of NKG2D.

Lack of Rap1 does not affect NK cell–mediated conjugate formation or cytotoxicity

NK cells recognize their target cells through the formation of supramolecular activation clusters (SMAC). LFA1 is a critical structural component of the peripheral SMAC, and the inability of LFA1 to polarize severely disrupted the SMAC formation (Mace et al., 2009). Our present study indicates that lack of Rap1a or Rap1b resulted in significantly reduced LFA1 polarization. Therefore, we next tested the ability of these NK cells to form conjugates with YAC-1 cells. NK cells (CFSE) and YAC-1 (TAMRA) were mixed at 1:1 ratio and incubated for different lengths of time. Our results indicate that lack of neither Rap1a nor Rap1b affected the ability of NK cells to recognize and form stable conjugates with YAC-1 cells (Fig. 3 B). Conjugate formation by NK cells lead to cytotoxicity. To determine the role of Rap1-GTPases in tumor killing, we next analyzed the NK-mediated cytotoxicity against EL4^{H60} and YAC-1 (H60+), CHO (hamster H2-D^{d}+), and BM-derived dendritic cells (BMDC; NCR1 ligand+). The cytotoxic potentials of NK cells were comparable and lack of Rap1a or Rap1b did not affect the cytotoxic potentials of NK cells (Fig. 3 C). Earlier studies have indicated that LFA1 may play a critical role in regulating this *'missing-self'* recognition (Barber et al., 2004). However, *Rap1a*$^{-/-}$ or *Rap1b*$^{-/-}$ NK cells showed similar levels of cytotoxicity against RMA/S cells (Fig. 3 C). As expected, there was only minimal lysis of EL4 or RMA by NK cells. Based on these results we conclude that the lack of Rap1 isoforms do not affect the NK-mediated cytotoxicity. Next, we evaluated the ability of Rap1b$^{-/-}$ mice to clear in vivo tumor growth (Fig. 3 D). Toward this, mice were intraperitoneally challenged with labeled RMA (CFSE) and RMA/S (TAMRA) cells. Clearance of RMA/S versus RMA cells was calculated compared with the input ratio, which was normalized to 1. RMA cells, which are not cleared by Rap1b$^{+/+}$ or Rap1b$^{-/-}$ mice acted as an internal control. Our results show that both Rap1b$^{+/+}$ and Rap1b$^{-/-}$ mice effectively cleared RMA/S cells, further confirming the ability of Rap1b$^{-/-}$ NK cells to mediate cytotoxicity.

Lack of Rap1b impairs cytokine/chemokine generation

Because NK cells regulate innate immune responses by generating multiple inflammatory cytokines and chemokines, we next investigated the role of Rap1 isoforms in their production. *Rap1a*$^{+/+}$, *Rap1b*$^{+/+}$, or *Rap1a*$^{-/-}$ NK cells generated optimal amounts of IFN-γ when activated via NKG2D (Fig. 4, A and B), Ly49D (Fig. 4 C), and NK1.1 (Fig. 4 D). However, *Rap1b*$^{-/-}$ NK cells were significantly impaired in generating IFN-γ (Fig. 4 and Fig. S4, A and B). Further, generation of GM-CSF or chemokines MIP1-α, MIP1-β, and RANTES from *Rap1b*$^{-/-}$ NK cells were also significantly reduced after NKG2D-mediated activation (Fig. 4 B). RasGRP2/CalDAG-GEF1 is an essential Rap1GEF in lymphocytes that depends on both Ca^{2+} and DAG for activation (Guo et al., 2001). PMA and ionomycin can activate RasGRP2/CalDAG-GEF1. To test whether cytokine generation is dependent on Rap1b, we activated the NK cells with PMA and ionomycin and analyzed the percent of intracellular IFN-γ+ NK cells (Fig. S4 A). PMA plus ionomycin did result in the generation of IFN-γ from *Rap1a*$^{+/+}$, *Rap1b*$^{+/+}$, and *Rap1a*$^{-/-}$ NK cells. However, *Rap1b*$^{-/-}$ NK cells failed to generate similar levels of IFN-γ. NKG2D-mediated activation of *Rap1b*$^{-/-}$ NK cells also showed similar reductions in intracellular IFN-γ^{+} cells (Fig. 4 B and Fig. S4 B). In addition, ex vivo activation of freshly isolated *Rap1b*$^{-/-}$ NK cells also contained reduced percentages of IFN-γ^{+} cells compared with that of *Rap1b*$^{+/+}$ (Fig. S5 A). We also found a significantly lower copy number of IFN-γ–encoding mRNA in spleen-derived *Rap1b*$^{-/-}$ NK cells after NKG2D activation (Fig. 4 E), indicating a defect

mice treated intraperitoneally with Con A were stained with anti-MOMA (red), anti-B220 (blue), and anti-NCR1 (green) and analyzed through confocal microscope. White boxes represent enlarged views. Top enlarged images represent NCR1^{+} NK cells (green) within the red pulp area. Bottom enlarged images represent NCR1^{+} NK cells (green) that have trafficked into the follicular region. (G) Total numbers of NCR1^{+} NK cells that have trafficked inside individual follicles (●-*Rap1b*$^{+/+}$, ●-*Rap1b*$^{-/-}$) and their averages (–) are shown. 20 individual follicles were analyzed for *Rap1b*$^{+/+}$ and *Rap1b*$^{-/-}$ mice. (H and I) RBC-depleted *Rap1b*$^{+/+}$ and *Rap1b*$^{-/-}$ splenocytes were labeled with CFSE and TAMRA, respectively and injected into *Rap1b*$^{+/+}$ recipient mice. 3 h later, cells from spleens of recipient mice were stained with anti-NK1.1-APC and anti-CD3-PE-Cy7. CD3^{-}NK1.1^{+} cells were gated and shown (H). (I) Bar graph represents the average ratio between the recovered Rap1b$^{+/+}$ and *Rap1b*$^{-/-}$ NK cells, after correction to the ratio of input cells. Data shown in H and I were obtained from four recipient mice. Data shown in A–I are one representative of three independent experiments.

at the transcriptional level. To exclude a generalized hyporesponsiveness of *Rap1b*$^{-/-}$ NK cells, we stimulated the NK cells with IL-12 and IL-18 that initiate the Tyk2/JAK2-mediated Stat4 pathway (Watford et al., 2004). NK cells from all the mice generated comparable levels of IFN-γ (Fig. 4 F), indicating that the *Rap1b*$^{-/-}$ NK cells are fully competent. Thus, only NKG2D, Ly49D, or NK1.1-mediated signaling pathways depend on Rap1b for cytokine and chemokine generations.

To establish the role of Rap1b in cytokine production under a pathological condition, we employed the mouse-adapted human influenza virus A/PR/8/34 (H1N1, PR8) and a murine lung-derived epithelial cell line, LA4. Recognition of viral hemagglutinin (HA) by NCR1 in NK cells results in the generation of IFN-γ (Guo et al., 2008). Therefore, we quantified IFN-γ in the supernatants of PR8-infected LA4/NK co-cultures as an indicator of NK cell activation. Fig. 4 G shows that although the *Rap1b*$^{+/+}$ NK cells could produce ample levels of IFN-γ, *Rap1b*$^{-/-}$ NK cells generated significantly lower levels of this cytokine. To further validate our observations, *Rap1b*$^{+/+}$ and *Rap1b*$^{-/-}$ mice were infected with 5,000 PFU of PR8 and IFN-γ–producing NK cells were quantified in lung sections. Fig. S5 (B and C) shows that *Rap1b*$^{-/-}$ NK cells have decreased ability to generate IFN-γ. These in vitro and in vivo defects were not caused by reductions in NCR1 expression, as its level was normal (Fig. S5 D). Taken together, these results demonstrate that Rap1b plays a crucial role in cytokine and chemokine generation.

Rap1b regulates the functions of IQGAP1-mediated signalosome

Both IQGAP1 and KSR1 have been shown to regulate the MAPK signaling cascades by functioning as scaffold proteins

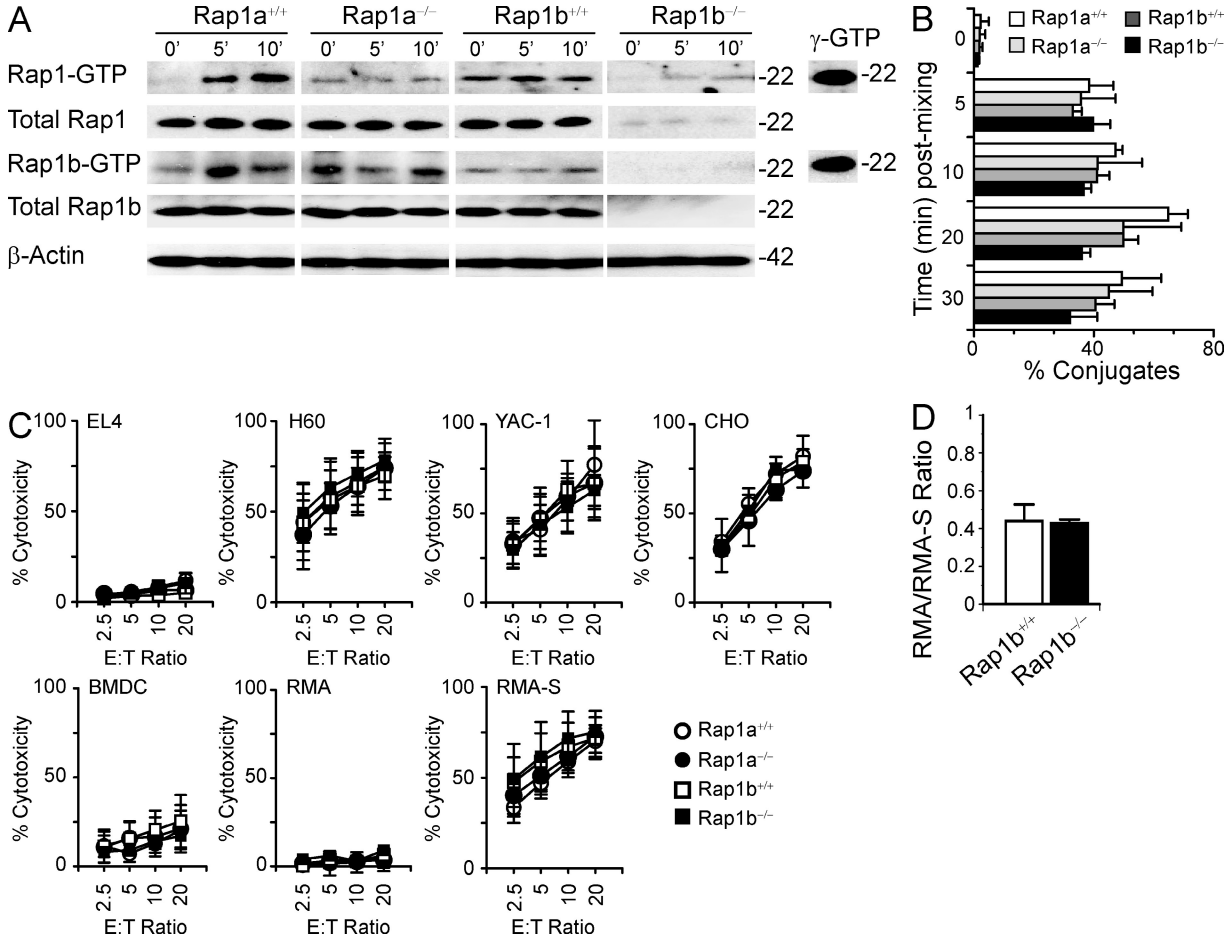

Figure 3. Stimulation via NKG2D activates Rap1 and lack of Rap1 does not affect NK cytotoxicity. (A) IL-2–cultured NK cells were activated with anti-NKG2D (A10; 5 µg/ml). Rap1-GTP was detected with anti-Rap1 or anti-Rap1b after pull-down. Total Rap1 or Rap1b proteins were quantified by analyzing the unfractionated NK cell lysates. A nonhydrolysable analogue of GTP, γGTPS, was also used to measure the total Rap1 and Rap1b. (B) NK cells (CFSE-labeled) and YAC-1 cells (TAMRA-labeled) were mixed at 1:1 ratio, and the double-positive conjugate percentages were quantified after fixing. (C) IL-2–activated splenic NK cells were incubated with [^{51}Cr]-labeled target cells at the indicated E:T ratios for 4 h. Three to five mice were used for each genotype. (D) RMA cells (TAMRA-labeled) and RMA/S cells (CFSE-labeled) were injected into mice and recovered peritoneal exudate cells were analyzed by flow cytometry. Clearance of RMA/S versus RMA cells was calculated compared with the input ratio, which was normalized to 1. RMA cells, which are not cleared by Rap1b$^{+/+}$ or Rap1b$^{-/-}$ mice acted as an internal control. Results presented in A–D are representative of three independent experiments.

(Razidlo et al., 2004; Royet al., 2005). To test the role of Rap1 in IQGAP1 or KSR1-mediated Raf/MEK1/2/ERK1/2 signalosome formation, we first tested their colocalization patterns. IL-2–cultured NK cells from *Rap1b*$^{+/+}$ and *Rap1b*$^{-/-}$ mice were stimulated with anti-NKG2D mAb (A10) for 15 min, fixed, and stained for Rap1, F-actin, and KSR1 or Rap1 and IQGAP1 proteins. Upon stimulation, KSR1 was predominantly localized to the luminal part of the peripheral membrane (Fig. S6, A and B). In contrast, Rap1b primarily localized throughout the cytoplasm and did not colocalize with KSR1. However, upon NKG2D-mediated activation, IQGAP1 and Rap1b colocalized closer to the perinuclear region of the cells (Fig. 5 A). In nonstimulated NK cells, IQGAP1 and Rap1b were distributed throughout the cytoplasm, indicating a redistribution of IQGAP1 after activation (Fig. S6 C). Co-localization of Rap1 and IQGAP1 was highly visible in the *Rap1b*$^{+/+}$ but not in *Rap1b*$^{-/-}$ NK cells.

Rap1b can regulate Rac1/Cdc42 activation via Vav-1 (Schwamborn and Püschel 2004). Rac1/Cdc42 in turn activate p21-activated kinase (Pak) that connects the upstream signaling to Rafs by phosphorylating S445 in B-Raf and S338 in C-Raf (Mason et al., 1999). Therefore, we next analyzed the levels of Vav-1 and Pak1/2/3 phosphorylation upon NKG2D-mediated activation (Fig. 5 B). Although there were no defects in Vav-1 phosphorylation, the level of Pak-1/2/3 phosphorylation were considerably reduced in *Rap1b*$^{-/-}$ NK cells (Fig. 5 C). Next, we examined the ability of B-Raf or C-Raf to associate with Rap1 and their phosphorylation status. To determine the level of Rap1 association, B-Raf was immunoprecipitated from lysates of NKG2D-activated *Rap1b*$^{+/+}$ NK cells and probed with anti-Rap1 or Rap1b antibodies. Because B-Raf exclusively associates with Rap1-GTP, the resulting protein band represents the activated form of Rap1. Fig. 5 D demonstrates the increase in the association of active Rap1-GTP, in particular Rap1b-GTP, to B-Raf with increasing time of activation. The ability of Rap1b-GTP to associate with C-Raf was analyzed in a pull down assay by the post-lysis mixing of recombinant GST–C-Raf–GRD fusion protein. Fig. 5 D shows increasing levels of Rap1-GTP or Rap1b-GTP associated to GST–C-Raf–GRD

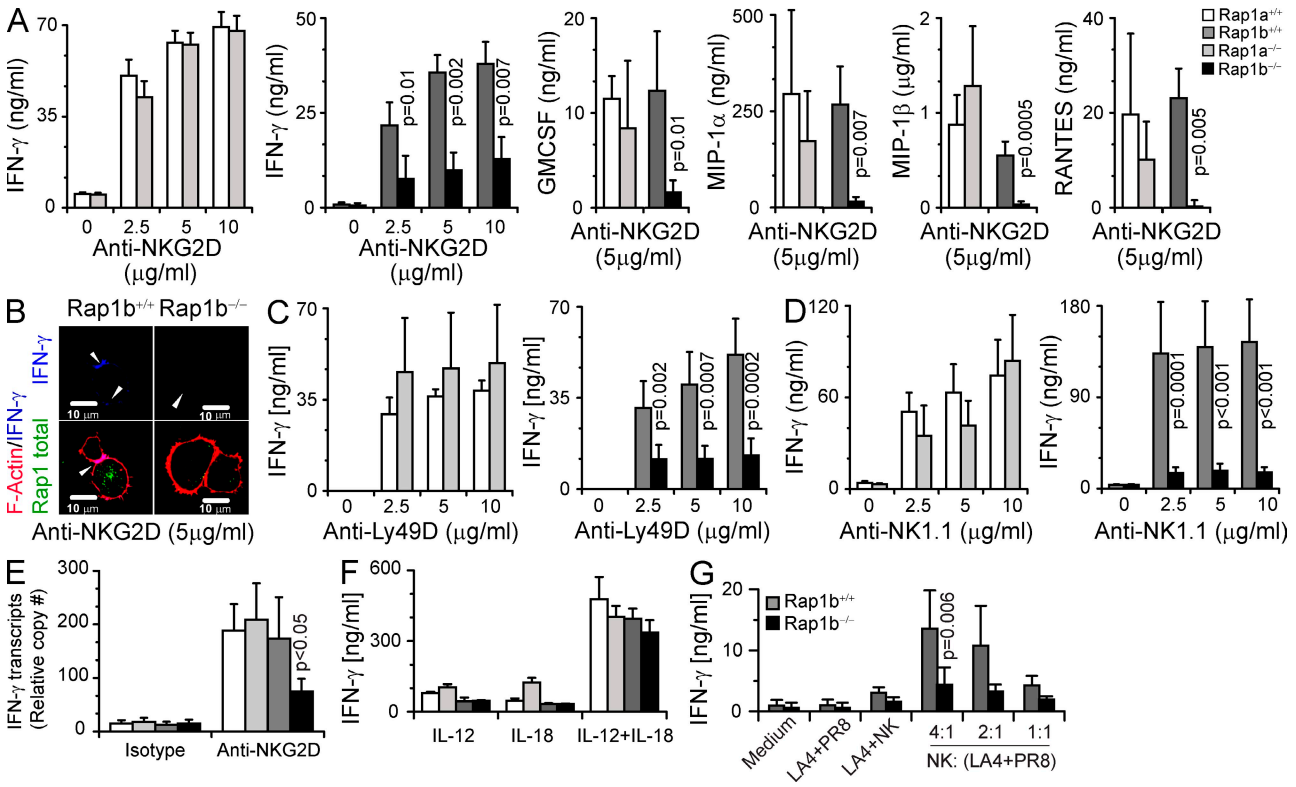

Figure 4. Lack of Rap1b results in reduced generation of cytokines and chemokines. (A) IL-2–cultured splenic NK cells (10^5 cells/well) were activated with anti-NKG2D (A10) and the supernatants were tested for cytokines or chemokines by ELISA and multiplex assays. Data presented are the mean with standard deviations from a minimum of 10 mice for each genotype from >3 independent experiments. (B) IL-2–cultured splenic NK cells were stimulated with anti-NKG2D (A10; 5 μg/ml). Activated CD3$^-$NK1.1$^+$ NK cells stained for intracellular IFN-γ (blue), F-actin (red), and Rap1 (green) and analyzed through confocal microscopy. Arrowheads mark IFN-γ. Data presented are representative images of >30 individual cells from 3 independent experiments. (C and D) NK cells were stimulated with anti-Ly49D (4E5; D) or anti-NK1.1 (PK136; D) and IFN-γ production was measured. (E) IFN-γ–encoding transcripts were quantified in splenic NK cells after anti-NKG2D stimulation. (F) IL-2–cultured NK cells were activated with IL-12, IL-18, or both (10 μg/ml) for 24 h and the supernatants were tested for the quantity of IFN-γ. (G) Splenic NK cells were co-cultured with LA4 cells with or without PR8 influenza, and IFN-γ was measured by multiplex assays after 16 h. Data presented in C–G were averages with standard deviations of three independent experiments.

with increasing activation time. Next, we stimulated NK cells via NKG2D to investigate the phosphorylation status of B-Raf and C-Raf (Fig. 5 E). Comparable amounts of both total B-Raf and C-Raf were present in *Rap1a*$^{+/+}$, *Rap1a*$^{-/-}$, *Rap1b*$^{+/+}$, and *Rap1b*$^{-/-}$ NK cells. However, upon activation, the phospho B-Raf (Serine 445) and C-Raf (Serine 338) were detectable only in *Rap1a*$^{+/+}$, *Rap1a*$^{-/-}$, and *Rap1b*$^{+/+}$ but not in *Rap1b*$^{-/-}$ NK cells. These observations were confirmed through confocal microscopy. Phospho B-Raf or C-Raf was drastically reduced in *Rap1b*$^{-/-}$ compared with *Rap1b*$^{+/+}$ NK cells (Fig. S7, A and B).

Activated B-Raf or C-Raf catalyzes the phosphorylation of MEK1/2, which in turn phosphorylates ERK1/2 (Yin et al., 2002). To identify the target MAP kinases, NKG2D-stimulated NK cells were analyzed for the phosphorylation levels of p38, JNK1/2, and ERK1/2. All three kinases were active in the *Rap1b*$^{+/+}$ NK cells. p38 and JNK1/2 phosphorylation were not affected in any of the NK cells tested (Fig. 5 F). However, the level of ERK1/2 phosphorylation was significantly reduced in *Rap1b*$^{-/-}$ NK cells (Fig. 5 F). These results are further validated by quantifying the intensity of phosphorylated proteins and comparing them with respective total proteins (Fig. S8 A). Furthermore, this reduction in ERK1/2 phosphorylation is not caused by a decrease in IQGAP1 protein in *Rap1b*$^{-/-}$ NK cells (Fig. S8 B). To visualize the fate of ERK1/2 activation in *Rap1b*$^{-/-}$ NK cells, we

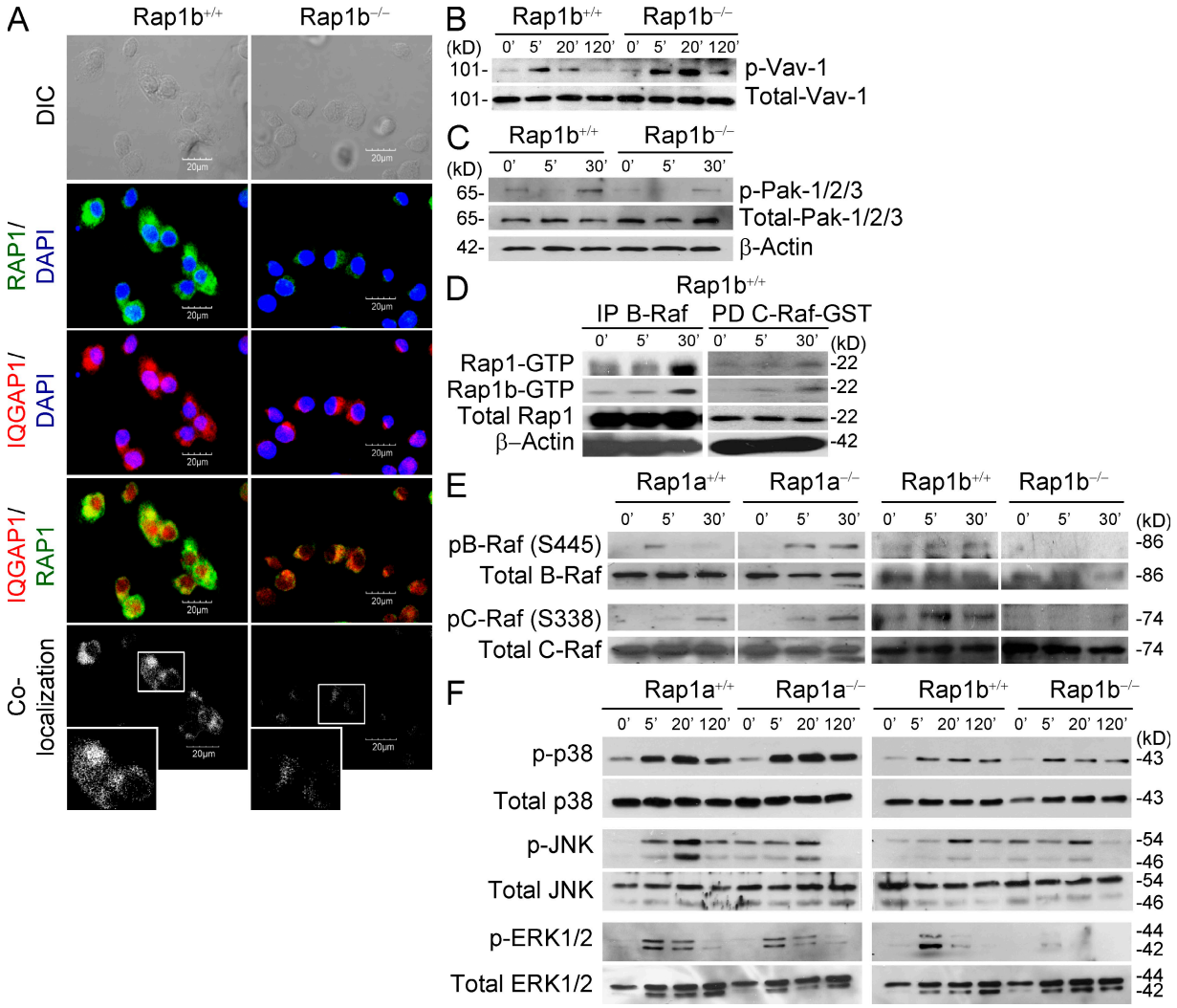

Figure 5. Rap1b regulates IQGAP1-mediated signaling cascade. (A) IL-2–cultured splenic NK cells were activated with anti-NKG2D for 30 min and stained for total Rap1 (green), IQGAP1 (red), and DAPI (blue) and analyzed by confocal microscopy. Inserts in the bottom panels are the enlarged views of the select NK cells. (B and C) NK cells from *Rap1b*$^{+/+}$ or Rap1b$^{-/-}$ mice were stimulated with anti-NKG2D for the indicated periods and the phosphorylation of Vav-1 (B) and Pak-1/2/3 (C) was analyzed. (D) IL-2–cultured splenic NK cells from *Rap1b*$^{+/+}$ mice were stimulated with anti-NKG2D (A10; 5 µg/ml). Cell lysates were subjected to immunoprecipitation (IP) with anti–B-Raf or pull down (PD) using recombinant GST-C-Raf. Resulting IP or PD were probed for the presence of Rap1-GTP or Rap1b-GTP. One representative experiment out of three is shown. (E and F) IL-2–cultured NK cells were stimulated with anti-NKG2D, and the cell lysates were analyzed for phospho and total proteins of B-Raf and C-Raf (E) or p38, JNK1/2, and ERK1/2 (F). Data presented in A–F were one representative of three independent experiments.

tracked their levels of phosphorylation through confocal microscopy (Fig. S8, C and D). Comparable levels of total ERK1/2 were present throughout *Rap1b*$^{+/+}$ and *Rap1b*$^{-/-}$ NK cells. Upon activation, significantly higher levels of phospho-ERK1/2 were seen in *Rap1b*$^{+/+}$ compared with *Rap1b*$^{-/-}$ NK cells. Thus, Rap1b was required for a sustained ERK1/2 phosphorylation. We further corroborated the role ERK1/2 activation in cytokine and chemokine generation using pharmacological inhibitors in wild-type *Rap1b*$^{+/+}$ NK cells. Inhibition of p38 or JNK1/2 caused minimal reduction in cytokine and chemokine generation. However, inhibition of MEK1/2 upstream of ERK1/2 completely ablated the generation of all the cytokines and chemokines in a dose-dependent manner (Fig. S8 E). We conclude that a sequential recruitment and phosphorylation of Raf→MEK1/2→ERK1/2 is regulated by Rap1b.

Rap1b facilitates the formation of IQGAP1-dependent signalosome

We next investigated the spatiotemporal organization of IQGAP1–Raf–ERK complexes during signal transductions. IL-2–cultured NK cells were stimulated via NKG2D and stained for IQGAP1 and ERK1/2. NKG2D-mediated activation resulted in IQGAP1-based large signalosome formation in the perinuclear region to coordinate the phosphorylation of ERK1/2. In nonstimulated NK cells, phospho-ERK was not detectable and the IQGAP1 was distributed throughout the cytoplasm with slight accumulation around the perinuclear region (Fig. 6 A). After 15 min of activation, ERK1/2 phosphorylation was evident *Rap1b*$^{+/+}$ NK cells. However, the level of ERK1/2 phosphorylation was less in *Rap1b*$^{-/-}$ NK cells. After 30 min of activation, the distribution pattern of IQGAP1 was drastically altered with a strong accumulation around the nucleus in *Rap1b*$^{+/+}$ NK cells. Although, IQGAP1 could accumulate around the nucleus in *Rap1b*$^{-/-}$ NK cells, signalosome was less pronounced. Arguably, a significant quantity of phospho-ERK1/2 colocalized with IQGAP1 in *Rap1b*$^{+/+}$ NK cells. In contrast, *Rap1b*$^{-/-}$ NK cells consistently showed reduced levels of phosphorylated ERK1/2 with no detectable IQGAP1 colocalization. These reduced ERK1/2 phosphorylation levels were not caused by a reduction in the total ERK1/2 level, because both *Rap1b*$^{+/+}$ and *Rap1b*$^{-/-}$ NK cells contained comparable levels of these proteins (Fig. 6 B). Thus, Rap1b is important for the spatiotemporal regulation of IQGAP1–ERK complexes. We conclude that Rap1b helps IQGAP1 to form a large signalosome in the perinuclear region of the NK cell, where transient but abundant phosphorylation of ERK1/2 occurred. Lack of Rap1b affected the structure of the IQGAP1-based signalosome and failed to support the phosphorylation of ERK1/2 (Fig. 7, A and B). Because LFA1 polarization and ICAM1-mediated spreading were defective in *Rap1b*$^{-/-}$ NK cells, we also tested the ability of anti-LFA1–mediated IQGAP1 protein redistribution. NK cells were activated with plate-bound anti-LFA1

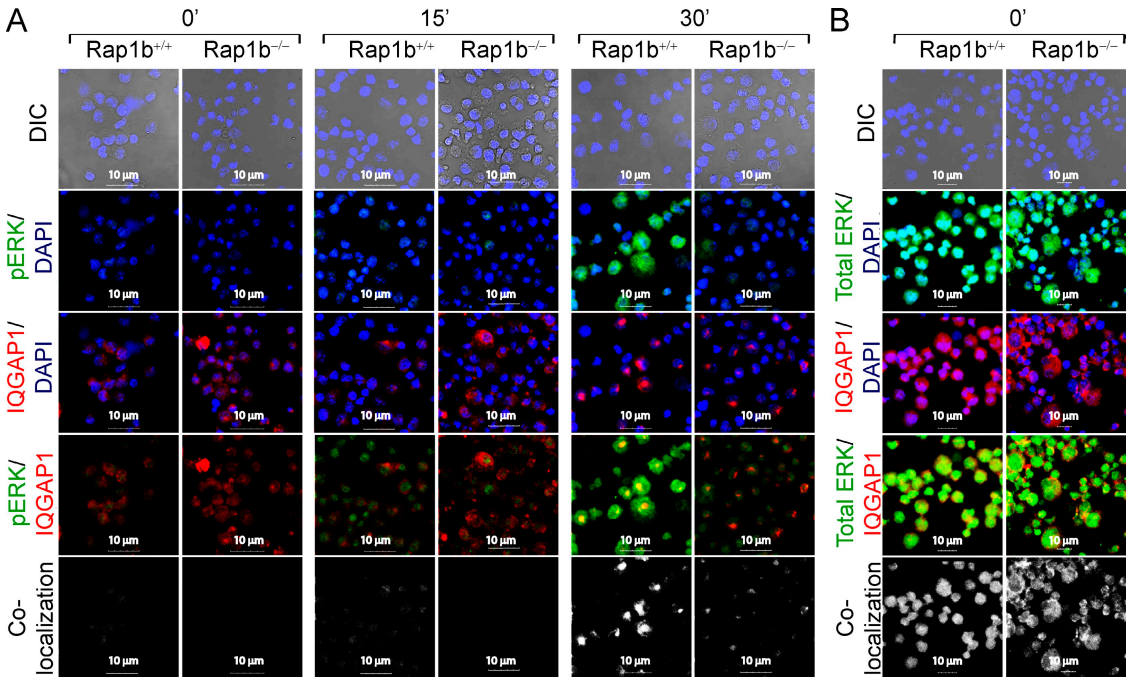

Figure 6. Rap1b regulates IQGAP1-mediated signalosome formation and ERK1/2 phosphorylation. (A) anti-NKG2D or (B) unstimulated splenic NK cells were stained for phospho ERK1/2 (green), IQGAP1 (red), and DAPI (blue), and analyzed by confocal microscopy. Data presented were one representative set from of >3 independent experiments.

mAb for the indicated times, fixed, and stained with anti-IQGAP1 mAb and DAPI (Fig. S8 F). We did not observe any redistribution of IQGAP1 even after 60 min of anti-LFA1 mAb-mediated activation in *Rap1b*$^{+/+}$ or *Rap1b*$^{-/-}$ NK cells. Thus, we conclude the signalosome formation and organization of MAPK signaling cascade are unique phenomena of activating receptors.

Rap1b regulates the proper formation MTOC

Earlier studies have shown that phospho-ERK2 localizes to the microtubules and regulates the polarization and directional translocation of MTOC to the NK immunological synapse (NKIS; Chen et al., 2006). Because ERK1/2 phosphorylations were reduced in *Rap1b*$^{-/-}$ NK cells, we next analyzed the formation of the MTOC. NK cells were activated via NKG2D and stained for α-tubulin and F-actin. Using confocal images, the lengths of the MTOCs were measured. Fig. 8 A shows representative NK cells and their measured MTOC lengths in multiple Z-stacks. These results indicate that lack of Rap1a or Rap1b did not affect the formation of the MTOC. However, the size and the length of MTOCs were proportionately much larger in *Rap1b*$^{-/-}$ NK cells compared with others. Analyses of the MTOCs at different Z-planes also revealed that the overall height and size of the MTOCs were considerably larger in *Rap1b*$^{-/-}$ NK cells (Fig. S9, A and B). Statistical significance was calculated by comparing the longitudinal length of the MTOCs to the maximal diameter of NK cells (Fig. 8 B). These results additionally emphasize that the lack of Rap1a or Rap1b did not alter the maximal NK cell lengths (Fig. S10). However, the lengths of MTOCs in *Rap1b*$^{-/-}$ NK cells are significantly larger compared with Rap1b$^{+/+}$ NK cells. *Rap1b*$^{-/-}$ NK cells also displayed multiple, noncomplete MTOCs (Fig. S9 A, arrows). Our results also show that a significant quantity of Rap1b colocalized to the center core of the MTOC in *Rap1b*$^{+/+}$ NK cells. Although, Rap1a was detectable in *Rap1b*$^{-/-}$ NK cells, it did not colocalize with the MTOC (Fig. 8 C).

DISCUSSION

Our results show that Rap1b is the major isoform in NK cells and its absence did not alter the development and terminal

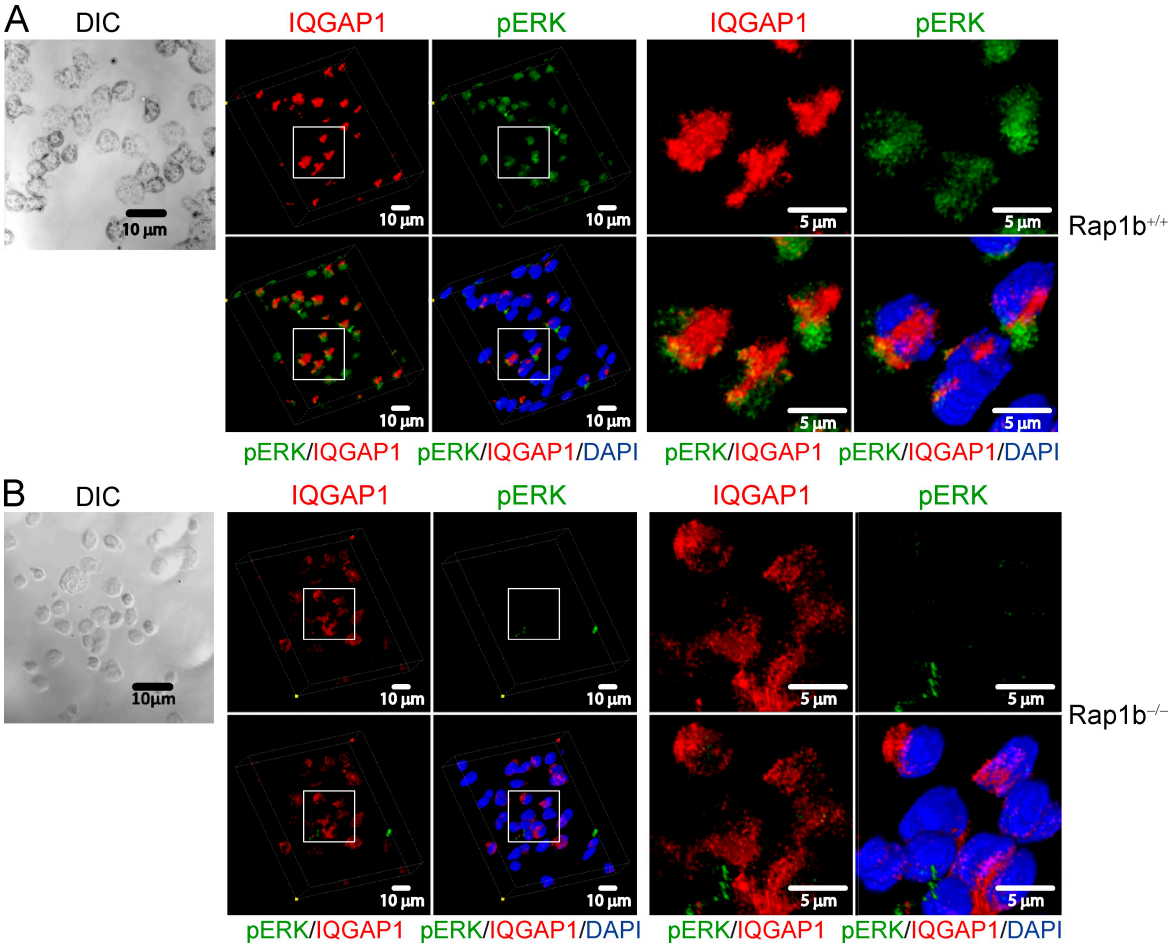

Figure 7. IQGAP1 mediates the formation of a large signalosome in the perinuclear region of the activated NK cells. IL-2–cultured splenic *Rap1b*$^{+/+}$ (A) and *Rap1b*$^{-/-}$ (B) NK cells were activated with anti-NKG2D (A10) for 30 min and stained for IQGAP1 (red), phospho-ERK1/2 (green), and DAPI (blue). Three dimensional reconstruction of images was done using 40 individual Z-stacks that were 0.4 µm thick, using FV1-ASW2.0 software. Data shown are one representative panel of 20 images analyzed from three independent experiments.

maturation of NK cells. Here, we present genetic evidence that Rap1b is a critical regulator of the IQGAP1-mediated signalosome formation. This signaling complex organized the sequential recruitment and phosphorylation of B-Raf or C-Raf and ERK1/2 in NK cells and was responsible for the cytokine and chemokine generation. Rap1b also played a crucial role in LFA1 polarization, cell spreading, and trafficking of NK cells. Lack of Rap1b, but not Rap1a, affected proper MTOC formation in NK cells.

Rap1 regulates LFA1-mediated cell adhesion (Stork and Dillon, 2005). LFA1 is a critical component of the SMAC in lymphocytes (Lin et al., 2005). Initial contact between NK and the target cells are mediated through the interactions between LFA1 and ICAMs followed by the recognition and binding of major receptors such as NKG2D to their respective ligands. A Rap1-dependent avidity modulation of low-affinity LFA1 into a conformationally active high-affinity adhesion molecule is critical for lymphocyte adhesion and trafficking (Dustin et al., 2004). Our study shows that absence of either Rap1a or Rap1b had significantly affected the polarization of LFA1 in NK cells. This reduced polarization also affected the ability of NK cells to bind and spread on anti-LFA1 mAb or recombinant ICAM1-Fc–coated plates. Thus, a defective affinity maturation of LFA1 could be the mechanistic explanation for the reduced adhesion of *Rap1b*$^{-/-}$ NK cells. This reduced LFA1 adhesion could be the basis for the defects in the emigration of *Rap1b*$^{-/-}$ NK cells from the spleen. Adaptive transfer experiments indicated that the *Rap1b*$^{-/-}$ NK cells can immigrate inside the recipient spleen; however, a higher percentage of *Rap1b*$^{-/-}$ NK cells failed to emigrate. Retention of a higher percentage of *Rap1b*$^{-/-}$ NK cells in *Rap1b*$^{+/+}$ spleen could also be caused by defects in other cell

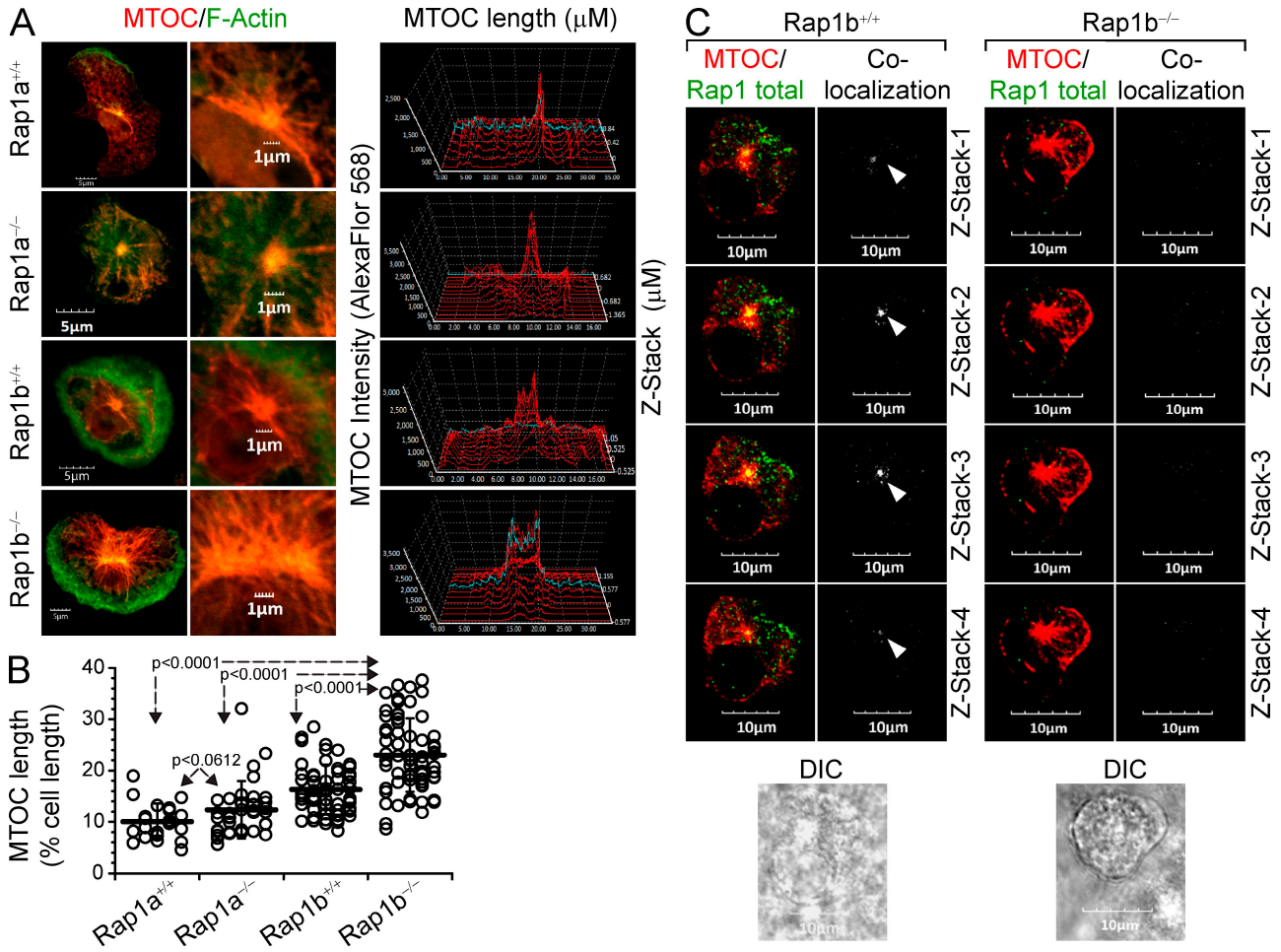

Figure 8. Rap1b colocalizes with MTOC and regulates its proper formation in NK cells. (A) NK cells from indicated mice were stimulated with anti-NKG2D (A10; 5 μg/ml) for 2 h and stained for α-tubulin (red) and F-actin (green). Data presented are one representative confocal image of 50 cells analyzed for each genotype. Precise sizes of MTOCs were measured by drawing a reference line across the longitudinal length of each NK cell. (B) Lengths of the MTOCs of NK cells from *Rap1a*$^{+/+}$ (n = 22), *Rap1a*$^{-/-}$ (n = 60), *Rap1b*$^{+/+}$ (n = 39), and *Rap1b*$^{-/-}$ (n = 67) were compared with their respective total cell length and presented as the percent of total cell length. (C) NK cells were stained for α-tubulin (red) and total Rap1 (green). Confocal images of NK cells at different z-planes with 0.4-μm intervals are shown. Arrowheads mark the colocalized Rap1 and MTOC. Data presented are representative images of >50 microscopic fields analyzed for each genotype from >3 independent experiments.

types that line the marginal sinuses. NK cells traffic in and out of the spleen through the MZ sinuses (Grégoire et al., 2008). The MZ is a continuous network of reticular fibroblasts in the red pulp area and MAdCAM-1$^+$ sinus lining cells. Metallophilic macrophages form a cell barrier immediately beneath the MAdCAM-1$^+$ sinus lining cells. Lack of Rap1a or Rap1b did not affect the total number of MOMA$^+$ MZ metallophilic macrophages; however, their distributions were extensively altered in the spleens of *Rap1b*$^{-/-}$ mice. Discontinuous linings and loss of a compact structure of metallophilic macrophages were evident in the *Rap1b*$^{-/-}$ mice. In addition, the total numbers of MZ B cells were significantly reduced in both *Rap1a*$^{-/-}$ and *Rap1b*$^{-/-}$ mice. Thus, loss of critical cell types that regulate the emigration of NK cells could be one of the major reasons for a higher number of NK cells retained in the spleen.

The loss of splenic architecture and a reduction in the MZ B cells in the spleens could also explain the failure of *Rap1b*$^{-/-}$ NK cells to enter into the T cell area after mitogenic stimulations. Under normal conditions, NK cells home inside the red pulp area at a steady-state and are excluded from the T and B cell–rich white pulp. However, during inflammation, NK cells traffic into the T cell area via MZ. The loss of MOMA$^+$ macrophage lining and a MZ B cell reduction could have resulted in a failure in the LFA1-mediated NK cell adhesion or a severe reduction in the generation and maintenance of a chemokine gradient (such as CXCR3 and CCL5). Irrespective of the LFA1 defects in *Rap1b*$^{-/-}$ NK cells, they were able to form successful conjugates with tumor cells and mediate anti-tumor responses against target cells both in vitro and in vivo. In addition, *Rap1b*$^{-/-}$ NK cells were also able to mediate moderate but comparable levels of cytotoxicity against syngeneic BMDCs. This indicates that the perforin/granzyme-containing cytotoxic granules do not depend on Rap1 for their movement to SMAC. However, it is also highly likely that a compensatory, shared functional ability of Rap1 isoforms could be the reason that neither *Rap1a*$^{-/-}$ nor *Rap1b*$^{-/-}$ NK cells demonstrated any cytotoxic defects. Generation of double knockout mice could definitively answer the role of Rap1 isoforms in NK-mediated cytotoxicity.

NK cells generate inflammatory cytokines and chemokines as part of innate immunity. A significant reduction in NKG2D, Ly49D, NK1.1, and NCR1-mediated cytokine and chemokine generation was observed in *Rap1b*$^{-/-}$ NK cells. This reduction was not caused by a generalized anergy because stimulation with optimal amounts of IL-12 and IL-18 resulted in comparable levels of IFN-γ between WT and *Rap1b*$^{-/-}$ NK cells. Thus, the ITAM-independent, Stat-dependent pathways are fully operational in *Rap1b*$^{-/-}$ NK cells. The explanation for this observation comes from the comparable levels of p38 phosphorylation between WT and *Rap1b*$^{-/-}$ NK cells, which is crucial for the generation of cytokines downstream of IL-12/IL-18 receptors (Berenson et al., 2006).

Defects in the cytokine/chemokine generation can be explained by three distinct functions of Rap1b (Fig. S11). First, Rap1b is known to bind and regulate Vav-1 that functions as a GEF for Rac1 and Cdc42 (Arthur et al., 2004). Our data indicates that the lack of Rap1b did not affect the phosphorylation of Vav-1. However, Vav isoforms are redundant in their ability to activate Rac1 and Cdc42 (Pearce et al., 2002) and the status of Vav-2 or Vav-3 in *Rap1b*$^{-/-}$ NK cells is yet to be determined. Downstream of Vav, Rac1, and Cdc42 are critical for the phosphorylation and recruitment of p21-activated kinase-1/2/3 (Pak-1/2/3) into the IQGAP1 scaffold. Our results show a reduction in the overall Pak activation. Therefore, lack of Rap1b could have affected the activation of one or more of Vav isoforms resulting in reduced Rac1 and Cdc42 activation and recruitment to the C-terminal GRD domain of IQGAP1. A reduction in Rac1/Cdc42 binding to IQGAP1 will affect the recruitment of Pak-1/2/3 to IQGAP1 complex. Because Pak-1/2/3 is responsible for the phosphorylation of B-Raf and C-Raf, any modulation of Pak-1/2/3 function would disrupt the sequential activation of B-Raf/C-Raf→MEK1/2→ERK1/2. ERK1/2 play a critical role in the activation and function of AP1, which could regulate the transcription of cytokine and chemokine genes (Chuang et al., 2001). Second, Rap1 could regulate IQGAP1 through its direct binding. Earlier studies have shown that both Rap1a-GTP and Rap1b-GTP bind equally to the IQ domain of IQGAP1 (Jeong et al., 2007). Interestingly, the IQ domain is also the site where B-Raf has been shown to be recruited (Ren et al., 2007). Thus, a lack of Rap1b could have affected the interaction between B-Raf and IQGAP1. Additional studies are required to delineate the functional relevance of this direct interaction between Rap1b to IQGAP1. Third, Rap1b can bind to B-Raf or C-Raf directly and regulate their functions. Previous studies (Guo et al., 2001) and our results demonstrate a direct interaction of Rap1b to B-Raf and C-Raf. This direct interaction could play a critical role in the autophosphorylation and stabilization similar to Ras-GTPases (Tran et al., 2005). Reduction in the phosphorylation of both B-Raf and C-Raf in *Rap1b*$^{-/-}$ NK cells demonstrates that Rap1-GTP plays a critical role in regulating their levels of phosphorylation, recruitment to IQGAP1, or both. Irrespective of its detectable levels, Rap1a did not rescue B-Raf and C-Raf phosphorylations in *Rap1b*$^{-/-}$ NK cells, indicating the exclusive role played by Rap1b. Additionally, it is possible that only Rap1b is capable of regulating the MAPK signaling cascade, as it is the major isoform in NK cells. Further, lack of Rap1a did not affect the normal levels of B-Raf or C-Raf phosphorylations after NKG2D-mediated activation. Thus, our data show a distinct functional dichotomy between the two Rap1 isoforms. Binding of Rap1a to IQGAP1 could regulate a distinct set of functions such as actin polymerization and maintenance of cell integrity. A defect in one or more of these three steps can negatively affect the sequential phosphorylations of Pak-1→Raf→MEK1/2→ERK1/2 in IQGAP1-mediated signalosome.

Although scaffolding proteins have been shown to regulate sequential phosphorylations, the spatiotemporal organization

and movement of signalosomes are not well understood. Our study shows an accumulation of IQGAP1 around the nucleus after NKG2D-mediated activation. The formation of this massive molecular complex was transient, but aided in the phosphorylation of ERK1/2. Lack of Rap1b did not alter the redistribution of IQGAP1 around the nucleus; however, the signalosomes were somewhat diffuse in *Rap1b*$^{-/-}$ NK cells with negligible levels of phospho-ERK1/2 around them. Activation with plate-bound anti-LFA1 mAb did not result in the formation of similar cellular structures, indicating a differential activation requirement. We propose that multiple signalosomes assemble to form the larger complex to facilitate the compartmentalized activation and phosphorylation of substrates in the perinuclear region of the activated cells. These signalosomes are predictably regulating multiple signaling cascades. NKG2D-mediated activation of *Rap1b*$^{+/+}$ NK cells resulted in a sustained ERK1/2 phosphorylation lasting for ~30 min within the signalosome; however, similar activations resulted only in a minimal and transient ERK1/2 phosphorylation lasting for only ~15 min in *Rap1b*$^{-/-}$ NK cells. Thus, a defect in IQGAP1-mediated signalosome function is one of the molecular explanations for the defects in cytokine and chemokine generations in *Rap1b*$^{-/-}$ NK cells. A structured signalosome may be required for the generation of transient but optimal functions of kinases. Support for such a hypothesis comes from the Ras-regulated ERK activation. EGF-induced Ras-mediated B-Raf–MEK1/2–ERK1/2 activation pathway required IQGAP1 for sequential kinase–substrate interactions (Yamaoka-Tojo et al., 2006). In this model, lack of IQGAP1 reduced B-Raf phosphorylation. Besides, IQGAP1-associated B-Raf contained much higher kinase activity, demonstrating a structural requirement for successful kinase–substrate interactions (Ren et al., 2007). Such an ordered regulation of kinases could be a critical integral part of IQGAP1-mediated signalosome that regulates NK cell functions.

The MTOC is the anchoring center of microtubules that regulates the intracellular trafficking of lytic granules. MTOC is made up of two centrioles that act as the core microtubule nucleation site (Basto et al., 2008). Our results indicate that the lack of Rap1b, but not Rap1a, resulted in a significant increase in the length and size of the MTOC. Additionally, few of the *Rap1b*$^{-/-}$ NK cells possessed 2 to 3 MTOCs that were distinct. Further, Rap1b predominantly colocalized to the MTOC region. A small but detectable level of Rap1a consistently localized throughout the cytoplasm, but not with MTOC. Earlier studies have indicated that polarization of lytic granules to the NKIS depends on proper MTOC function (Orange et al., 2003). Normal levels of cytotoxic potential by *Rap1a*$^{-/-}$ or *Rap1b*$^{-/-}$ NK cells in the present study indicate that movement of lytic granules is not regulated by the lack of Rap1b. Improper formation of the MTOC was not the reason for the defective cytokines generation from *Rap1b*$^{-/-}$ NK cells. Our study demonstrates a significant reduction in the IFN-γ encoding mRNA in *Rap1b*$^{-/-}$ NK cells, which points to a defect at the transcriptional regulation rather than a blockade in the secretory pathway. Defects in MTOC formation could have resulted for multiple reasons. Lack of Rap1b resulted in reduced ERK1/2 phosphorylation that could have affected the proper formation of the MTOC. This is in line with earlier studies that have shown that phospho-ERK2 localizes to the microtubules and inhibitors to MEK1/2 severely affected the remodelling of microtubules (Chen et al., 2007). Other studies have shown that the function of Cdc42 required the sequential activation of Rap1b in axonal elongation (Schwamborn and Püschel, 2004). In this context, an indirect regulation of Cdc42 or Rac1 by Rap1b via Vav1 (Maillet et al., 2003) could be responsible for improper formation of tubulin oligomerization and MTOC formation.

In summary, our study demonstrates that signal processing by IQGAP1 scaffold requires Rap1b-GTPase. Lack of Rap1b affected the sequential phosphorylation and activation of PAK1→Raf→MEK1/2→ERK1/2 cascade in IQGAP1-mediated signalosome. IQGAP1 also recruits signaling proteins such as β-catenin, E-cadherin, CLIP, and APC. Future studies will provide insights into the role of Rap1-GTPases in regulating these additional signaling cascades.

MATERIALS AND METHODS

Mice and cells. Generation of *Rap1a*$^{-/-}$ (Li et al., 2007) and *Rap1b*$^{-/-}$ (Chrzanowska-Wodnicka et al., 2005) mice was previously described. *Rap1a*$^{-/-}$ and *Rap1b*$^{-/-}$ mice were backcrossed with C57BL/6 strain for >*n*11 generations. These strains were maintained by heterozygote × heterozygote breeding to obtain knockouts (*Rap1a*$^{-/-}$ and *Rap1b*$^{-/-}$) and wild-type littermate controls (*Rap1a*$^{+/+}$ and *Rap1b*$^{+/+}$). All the animal protocols were approved by the Institutional Animal Care and Use Committee, Biological Resource Center, and Medical College of Wisconsin. EL4, EL4^{H60}, RMA/S, LA4, and MDCK cell lines were previously described (Guo et al., 2009). BMDCs were generated from 129J mice following established protocols (Lutz et al., 2000).

NK cell preparation. NK cells were prepared as previously described (Awasthi et al., 2008). Briefly, single-cell suspensions from spleen and BM were passed through nylon wool columns to deplete adherent populations consisting of B cells and macrophages. Nylon wool-nonadherent cells were cultured with 1,000 U/ml of IL-2 (NCI-BRB-Preclinical Repository). IL-2–cultured NK cells were used on day 6. Purity of the NK cultures was checked, and preparations with >90% of NK1.1^{+} cells were used.

Flow cytometry. Single cell preparations from spleen, BM, thymus, or IL-2–cultured NK cells (sixth day) were stained and analyzed as previously described (Regunathan et al., 2006). Flow cytometry analysis was performed in LSR-II and analyzed with FACSDiva software (BD). Antibodies for the following were used: B220 (RA3-6B2), IgM (R6-60.2), IgD (11-26c.2a), CD19 (1D3), CD1d (1B1), CD21/CD35 (4E3), CD23 (B3B4), CD3ε (145-2C11), CD16/CD32(93), NK1.1 (PK136), NKG2D (A10), NKG2A (16a11), CD43 (1B11), CD49b (DX5), CD51 (RMV-7), CD122 (5H4), CD11b (M1/70), CD27 (LG.7F9), and Ly49I (YLI-90; all from eBioscience); CD4 (H129.19), CD8 (53–6.2), Ly49A (A1), Ly49D (4E5), and Ly49C/I (5E6; all from BD); MOMA-1-FITC (Serotec); IgM F(ab′)$_2$ (Jackson ImmunoResearch Laboratories). CFSE (C-1157) and TAMRA (C-300; both from Sigma-Aldrich) were used to label NK cells.

Immunofluorescence microscopy. Spleens were embedded in OCT using Tissue-Tek trays (Sakura Finetek), frozen with a dry-ice/Isopropanol mixture, and kept at −80°C until sectioning. 7-μm cryostat sections were generated, air-dried for 1 h at room temperature, and fixed in acetone for 10 min. The sections were blocked with 0.1% BSA/PBS containing anti-CD16/CD32

mAb for 45 min, washed, and incubated for 1 h at room temperature with the rat anti–mouse MOMA-1 and anti-NCR1 antibodies followed by Alexa Fluor–conjugated secondary antibodies. Sections were mounted in aqueous mounting medium and visualized on inverted Nikon Eclipse TE200 fluorescence microscope. Images were taken at 20× magnification.

Confocal microscopy. Confocal analyses were performed in Olympus FluoView FV1000 MPE microscope that is equipped with multiphoton capabilities (MaiTai DSBB-OL, 710–990 nm; MaiTai DSHP-OL, 690–1,040 nm). NK cells were activated in the presence of plate-bound anti-NKG2D mAb (A10; 5 μg/ml) or anti-LFA1 mAb (M1714; 5 μg/ml) at 37°C for indicated time points. Activated cells were harvested and plated in poly-L-lysine–coated (Sigma-Aldrich) LabTak chamber slides (Thermo Fisher Scientific). Cells were fixed/permeabilized with 4% paraformaldehyde for 15 min and blocked for 1 h with 3% BSA and 0.1% Triton X-100 in sterile PBS. Wherever required, NK cells were blocked with anti-CD16/CD32 mAb (BD) for 20 min. Staining with primary antibodies was performed for overnight at 4°C. The following dilutions of reagents were used: anti–total-Rap1, 1:200; anti-IQGAP1, 1:100; Anti-Rap1b, 1:100; anti-phospho C-Raf, 1:100; anti-total C-Raf, 1:100; anti-phospho B-Raf, 1:100; anti-total B-Raf, 1:100; anti-total ERK1/2, 1:100; anti-phospho ERK1/2, 1:100; anti-Tubulin, 1:200; anti-Rap2, 1:200; anti-KSR1, 1:200; anti-NCR1, 1:100; anti-IFN-γ-PE, 1:50; anti-LFA1, 1:200; mAbs, Phalloidin-Red (F-actin), 1:1000; Lysotracker Red, 1:500; and DAPI, 1:1000. Alexa Fluor–conjugated secondary antibodies were used at a 1:2,000 dilutions. Stained slides were mounted with Vectashield mounting medium (Vector Laboratories) and images were taken with a 40× or 100× oil immersion lenses. Z-stacks were acquired using Olympus software. Multiple (40–70) Z stack of 0.4-μm slice were acquired for three-dimensional analysis analysis. Three-dimensional projections were generated by compiling 40 Z-stack images.

LFA1 polarization and NK cell spreading. LFA1 polarization was quantified in IL-2–cultured NK cells (6 d) after PMA (10 mM) and ionomycin (10 mM) activation (37°C for 30 min). Cells were fixed/permeabilized with 0.1% Triton X-100 for 5 min, blocked with goat serum, stained with anti-LFA1 and Alexa Fluor 633–conjugated with secondary anti–mouse mAbs along with phalloidin red. Cells were washed and mounted in Vectashield. Localization of LFA1 in a focal point that is less than one fourth of the cell's total diameter was taken as successful polarization. NK cell spreading assays were performed in 96-well plate (Nunc) that were coated with isotype control (IgG), anti-LFA1 (M17/4), anti-NKG2D (A10) mAbs (each 5 μg/ml), or recombinant ICAM1-Fc (5 μg/ml). Plates were washed and IL-2–cultured NK cells (6 d; 10^5 cells/well) were added and incubated for 4 h at 37°C. Spreading of NK cells were observed in phase-contrast Nikon Eclipse TE200 microscope. Images were taken in the bright field using the Metamorph Imaging 6.1 software at 20× magnification. Spread NK cells were defined as the ones that lacked clearly visible edges.

In vivo NK cell trafficking and homing. Trafficking of NK cells from the red pulp area into the T/B rich white pulp area was performed using Con A (Sigma-Aldrich). *Rap1b*$^{+/+}$ and *Rap1b*$^{-/-}$ mice were intraperitoneally administrated with 500 μg of Con A in 200 μl of sterile PBS. Spleens were harvested after 8 h, mounted in OCT and sections (7 μm) were stained with anti–MOMA-FITC (1:200) and anti-NCR1 (1:100) mAbs. Confocal microcopy was used to quantify the number of NK cells trafficked into the white pulp area. For NK cell homing, RBC-depleted splenocytes from *Rap1b*$^{+/+}$ and *Rap1b*$^{-/-}$ were labeled with 2 μM CFSE or 10 μM TAMRA (Sigma-Aldrich). A mixture of 20×10^6 CFSE or TAMRA-labeled cells were injected intravenally into recipient *Rap1b*$^{+/+}$ mice. After 3 h, splenocytes from the recipient mice and labeled non-injected splenocytes were stained with anti-NK1.1 and CD3-PE-Cy7 mAbs. The homing efficiencies of Rap1b$^{-/-}$ and Rap1b$^{+/+}$ NK cells were calculated compared with the input ratio that was normalized to 1.

Cytotoxicity assays and in vivo tumor clearance. NK-mediated cytotoxicity was quantified using [^{51}Cr]-labeled target cells at varied E:T Ratio. Percent specific lysis was calculated using amounts of absolute, spontaneous, and experimental [^{51}Cr]-release from target cells. For the in vivo tumor clearance assay, RMA and RMA/S cells were labeled with 0.1 μM CFSE and 0.2 μM TAMRA (Invitrogen), respectively for 10 min and quenched with 10% FBS 1640 medium. Cells were mixed at a concentration of 10×10^6 cells/ml of each in PBS and 400 μl was injected intraperitoneally into each mouse. Peritoneal exudate was collected 8 h later, and the fluorescence of single-cell suspensions was analyzed by flow cytometry. The ratio of RMA/S to RMA cells was calculated. Clearance of RMA/S versus RMA cells was calculated compared with the input ratio, which was normalized to 1.

Conjugate formation. NK-target cell conjugate formation was measured by cytometry as described previously. NK cells (Rap1a$^{+/+}$, Rap1a$^{-/-}$ and Rap1b$^{+/+}$, Rap1b$^{-/-}$) and target cells (YAC-1) were labeled with CFSE (Invitrogen) or TAMRA (Invitrogen). Effector and target cells were mixed with 1:1 ratio in 100 μl of PBS. Mixed cells were centrifuged at 4°C for 3 min at 500 rpm and incubated at 37°C for indicated time periods. Cells were fixed by 0.5% formalin in PBS and analyzed by flow cytometry. Double positive cells were gated and the percentages of NK cells in the conjugates were quantified.

Viral infections and co-culture experiments. Mouse-adapted human influenza virus A/PR/8/34 (H1N1) was obtained from T. Moran, Department of Microbiology, Mount Sinai School of Medicine, New York. *Rap1b*$^{+/+}$ or *Rap1b*$^{-/-}$ mice were infected intranasally with 5000 PFU of PR8. Lungs were isolated from infected mice on day 7 of post infection to generate cryosections that were stained with anti-IFN-γ and anti-NCR1 mAbs. Co-culture assays were performed as described (Guo et al., 2008). LA4 cells (2.5×10^5 cell/well) were seeded in 24-well tissue culture plates for overnight and inoculated with PR8 at an MOI of 0.05. After 1 h incubation at 37°C, inoculums were removed and LA4 cells were washed twice, followed by the addition of IL-2–cultured splenic NK cells (6 d) at the indicated E:T ratio. Supernatants were collected after 18 h for IFN-γ quantification by ELISA.

Cytokine and chemokine quantification. IL-2–cultured, Fc-blocked NK cells were activated with titrated concentrations of plate-bound anti-NKG2D (A10), anti-Ly49D (4E5), and anti-NK1.1 (PK136) mAbs with indicated concentrations. Fresh NK cells from the spleen were isolated using anti-CD49b (DX5)-conjugated MicroBeads (Miltenyi Biotec) and activated with plate-bound anti-NK1.1 (PK136) mAb. NK cells were also activated with IL-12 (2.5 ng/ml), IL-18 (2.5 ng/ml) or both. IFN-γ, GM-CSF, MIP-1α, MIP-1β, and RANTES were quantified using Multiplex kit (Bio-Rad Laboratories). Intracellular cytokines were quantified using established methodologies (Malarkannan et al., 2007). Briefly, NK cells were activated with 5 μg/ml plate-bound anti-NKG2D (A10) mAb for 12 h in the presence of Brefeldin-A for the last 4 h of activation. Activated NK cells were blocked with anti-CD16/CD32, stained for NK1.1, fixed, permeabilized, and quantified for intracellular IFN-γ through flow cytometry. For IFN-γ-encoding mRNA quantification, NK cells were activated for 6 h and used for RNA extraction (RNeasy Mini Kit; QIAGEN). Real-time PCR was performed by using a previously published SYBR green protocol with an ABI7900 HT thermal cycler. Transcript in each sample was assayed in triplicates and the mean cycle threshold was used to calculate the *x*-fold change and control changes for each gene. Three housekeeping genes were used for global normalization in each experiment (*Actin*, *Rps11*, and *Tubulin*). Primer sequences for *IFN-γ* were 5′-GACTGTGATTGCGGGGTTGT-3′ (sense) and 5′-GGCCCGGAGTGTAGACATCT-3′ (anti-sense).

Pull-down, immunoprecipitation, and Western blotting. IL-2–cultured NK cells (sixth day) were stimulated with anti-NKG2D mAb (A10; 5 μM/ml) for indicated time points at 37°C or left unstimulated. Stimulation was terminated by adding 1 vol of 2× ice-cold lysis buffer (100 mM Tris, pH 7.4, 150 mM NaCl, 2% NP-40, 1% deoxycholic acid, 0.2% SDS, and 2 mM sodium orthovanadate with phosphatase inhibitor cocktail, PhosSTOP

[Roche] and proteinase inhibitor cocktail (Sigma-Aldrich). Lysates were incubated for 30 min on ice, centrifuged at 15,000 g for 15 min at 4°C. An aliquot of cell lysates (10^6 cell equivalent) was taken out to evaluate the total Rap1 protein. The remaining cell lysates were incubated with glutathione-agarose beads that precoupled with GST-RalGDS-RBD at 4°C. This assay is based on the fact that RalGDS binds with high affinity to Rap1-GTPase, but not to Rap1-GDP. The beads were washed and 30 µl of 1× Laemmli buffer was added and boiled at 95°C to elute the pulled-down proteins. The active Rap1 was analyzed by an antibody that recognizes both Rap1a and Rap1b. For Western blotting, cell lysate aliquot (corresponding to 1×10^6 cells) or pull-down protein pellets were resolved by SDS-PAGE, transferred to PVDF membranes, and probed with primary and the secondary antibodies. The signal was detected by ECL (GE Healthcare). Immunoprecipitation with anti–B-Raf mAb or pull-down with GST-C-Raf were performed to determine the association of Rafs with Rap1 proteins. NK cells were activated with plate-bound anti-NKG2D mAb (A10, 5 µg) for the indicated length of time and lysates were generated as described above. For B-Raf immunoprecipitation, NK cell lysates were precleared and incubated with anti–B-Raf mAb (Cell Signaling Technology) and protein-G beads overnight at 4°C. For C-Raf pull-down, NK cell lysates were incubated with glutathione-agarose beads that are precoupled with GST-C-Raf at 4°C for overnight. Glutathione or Protein-G beads were washed with 1× RIPA buffer (Boston BioProducts), and bound proteins were eluted with 30 µl of 1× Laemmli buffer, boiled at 95°C, and loaded onto 12% SDS-PAGE gels, transferred to PVDF membranes and probed with anti-total Rap1 (Santa Cruz Biotechnology, Inc.) and anti-Rap1b antibodies (Cell Signaling Technology). Blots were reprobed with anti–β-actin mAb. For Western blot analyses, NK cell lysates (1×10^6) were resolved using 10% SDS-PAGE gels and transferred to PVDF membranes. The blots were probed with following antibodies: rabbit anti–total Rap1 (Santa Cruz Biotechnology, Inc.), anti-Rap1a (Cell Signaling Technology), rabbit anti-Rap1b (Cell Signaling Technology), anti-GST mAb (Santa Cruz Biotechnology, Inc.), anti–phospho-Vav-1 (Y160; Abcam), anti–phospho-PAK1/2/3 (S141; Abcam), anti–phospho-p38 (Thr180/Tyr182; Cell Signaling Technology), anti–phospho-ERK1/2 (Thr202/Tyr204; Cell Signaling Technology), anti-phospho-JNK1/2 (Thr183/Tyr185; Cell Signaling Technology), anti–total Vav-1 (Cell Signaling Technology), anti–total PAK1/2/3 (Millipore), anti–total p38 (Cell Signaling Technology), anti–total ERK1/2 (Cell Signaling Technology), anti-total JNK1/2 (Cell Signaling Technology), anti-IQGAP1 (BD), and anti–β-Actin (Millipore) mAbs. Recombinant Rap1a-GST (full-length) and Rap1b-(85-184aa)-GST proteins (Novus Biologicals) were used as controls. Anti–phospho B-Raf (S445; Cell Signaling Technology), anti–phospho C-Raf (S338; Millipore), anti–total B-Raf (Cell Signaling Technology), and anti–total C-Raf (Cell Signaling Technology) were used in both Western blot and confocal analyses. Intensities of phospho protein bands were measured and compared with their respective total proteins using Adobe Imager.

Drug inhibition assay. Specific inhibitors for p38 (SB 202190), JNK1/2 (SP600125), and MEK1/2 (U0126; Sigma-Aldrich) were used. NK cells were pretreated with inhibitors for 1 h at 37°C, washed, and added to anti-NKG2D mAb (A10; 5 µg/ml)–coated plates. Plates were incubated for 18 h, and then supernatants were tested for cytokines and chemokines in a multiplex assay.

Statistics. Statistical analyses were performed by two-tail, unpaired, Student's *t* test. P values that are ≤ 0.05 were considered significant.

Online supplemental material. Fig. S1 shows subcellular localization of Rap1 and phenotypic characterization of T, NKT, and NK cells. Fig. S2 shows the development of NK cells in the absence of Rap1 isoforms. Fig. S3 shows the development of T and B cells in the absence of Rap1 isoforms. Fig. S4 shows that IFN-γ^+ production in *Rap1b*$^{-/-}$ NK cells are significantly reduced. Fig. S5 shows that ex vivo and in vivo generation of IFN-γ is defective in Rap1b$^{-/-}$ mice. Fig. S6 shows co-localization of Rap1 with KSR1 or IQGAP1. Fig. S7 shows NKG2D-mediated Raf phosphorylation in NK cells. Fig. S8 shows that ERK1/2 phosphorylation is critical for cytokine and chemokine generation. Fig. S9 shows MTOC formation in NK cells in the absence of Rap1 isoforms. Fig. S10 is a comparison of MTOC length with total cell length. Fig. S11 shows that Rap1b regulates IQGAP1-mediated signalosome formation. Online supplemental material is available at http://www.jem.org/cgi/content/full/jem.20100040/DC1.

We thank Hailong Guo, Pawan Kumar, and Ravi Lella of our laboratory for discussion and technical help.

A. Awasthi is supported by MCW-Cancer Center Postdoctoral Fellowship. This work is supported in part by ACS Scholar grant RSG-02-172-LIB; ROTRF grant # 111662730; and NIH grants R01 A1064826-01 (to S. Malarkannan); and an AHA grant 0950118G (to M. Chrzanowska-Wodnicka).

The authors claim no financial conflict of interest.

Submitted: 5 January 2010
Accepted: 27 July 2010

REFERENCES

Arthur, W.T., L.A. Quilliam, and J.A. Cooper. 2004. Rap1 promotes cell spreading by localizing Rac guanine nucleotide exchange factors. *J. Cell Biol.* 167:111–122. doi:10.1083/jcb.200404068

Awasthi, A., A. Samarakoon, X. Dai, R. Wen, D. Wang, and S. Malarkannan. 2008. Deletion of PI3K-p85alpha gene impairs lineage commitment, terminal maturation, cytokine generation and cytotoxicity of NK cells. *Genes Immun.* 9:522–535. doi:10.1038/gene.2008.45

Barber, D.F., M. Faure, and E.O. Long. 2004. LFA-1 contributes an early signal for NK cell cytotoxicity. *J. Immunol.* 173:3653–3659.

Basto, R., K. Brunk, T. Vinadogrova, N. Peel, A. Franz, A. Khodjakov, and J.W. Raff. 2008. Centrosome amplification can initiate tumorigenesis in flies. *Cell.* 133:1032–1042. doi:10.1016/j.cell.2008.05.039

Berenson, L.S., J. Yang, B.P. Sleckman, T.L. Murphy, and K.M. Murphy. 2006. Selective requirement of p38alpha MAPK in cytokine-dependent, but not antigen receptor-dependent, Th1 responses. *J. Immunol.* 176:4616–4621.

Chen, X., D.S. Allan, K. Krzewski, B. Ge, H. Kopcow, and J.L. Strominger. 2006. CD28-stimulated ERK2 phosphorylation is required for polarization of the microtubule organizing center and granules in YTS NK cells. *Proc. Natl. Acad. Sci. USA.* 103:10346–10351. doi:10.1073/pnas.0604236103

Chen, X., P.P. Trivedi, B. Ge, K. Krzewski, and J.L. Strominger. 2007. Many NK cell receptors activate ERK2 and JNK1 to trigger microtubule organizing center and granule polarization and cytotoxicity. *Proc. Natl. Acad. Sci. USA.* 104:6329–6334. doi:10.1073/pnas.0611655104

Chrzanowska-Wodnicka, M., S.S. Smyth, S.M. Schoenwaelder, T.H. Fischer, and G.C. White II. 2005. Rap1b is required for normal platelet function and hemostasis in mice. *J. Clin. Invest.* 115:680–687.

Chu, H., A. Awasthi, G.C. White II, M. Chrzanowska-Wodnicka, and S. Malarkannan. 2008. Rap1b regulates B cell development, homing, and T cell-dependent humoral immunity. *J. Immunol.* 181:3373–3383.

Chuang, S.S., P.R. Kumaresan, and P.A. Mathew. 2001. 2B4 (CD244)-mediated activation of cytotoxicity and IFN-gamma release in human NK cells involves distinct pathways. *J. Immunol.* 167:6210–6216.

de Rooij, J., F.J. Zwartkruis, M.H. Verheijen, R.H. Cool, S.M. Nijman, A. Wittinghofer, and J.L. Bos. 1998. Epac is a Rap1 guanine-nucleotide-exchange factor directly activated by cyclic AMP. *Nature.* 396:474–477. doi:10.1038/24884

Dustin, M.L., T.G. Bivona, and M.R. Philips. 2004. Membranes as messengers in T cell adhesion signaling. *Nat. Immunol.* 5:363–372. doi:10.1038/ni1057

Gotoh, T., S. Hattori, S. Nakamura, H. Kitayama, M. Noda, Y. Takai, K. Kaibuchi, H. Matsui, O. Hatase, H. Takahashi, et al. 1995. Identification of Rap1 as a target for the Crk SH3 domain-binding guanine nucleotide-releasing factor C3G. *Mol. Cell. Biol.* 15:6746–6753.

Grégoire, C., C. Cognet, L. Chasson, C.A. Coupet, M. Dalod, A. Reboldi, J. Marvel, F. Sallusto, E. Vivier, and T. Walzer. 2008. Intrasplenic trafficking of natural killer cells is redirected by chemokines upon inflammation. *Eur. J. Immunol.* 38:2076–2084. doi:10.1002/eji.200838550

Guo, F.F., E. Kumahara, and D. Saffen. 2001. A CalDAG-GEFI/Rap1/B-Raf cassette couples M(1) muscarinic acetylcholine receptors to the

activation of ERK1/2. *J. Biol. Chem.* 276:25568–25581. doi:10.1074/jbc.M101277200

Guo, H., A. Samarakoon, B. Vanhaesebroeck, and S. Malarkannan. 2008. The p110 delta of PI3K plays a critical role in NK cell terminal maturation and cytokine/chemokine generation. *J. Exp. Med.* 205:2419–2435. doi:10.1084/jem.20072327

Guo, H., P. Kumar, T.M. Moran, A. Garcia-Sastre, Y. Zhou, and S. Malarkannan. 2009. The functional impairment of natural killer cells during influenza virus infection. *Immunol. Cell Biol.* 87:579–589. doi:10.1038/icb.2009.60

Hart, M.J., M.G. Callow, B. Souza, and P. Polakis. 1996. IQGAP1, a calmodulin-binding protein with a rasGAP-related domain, is a potential effector for cdc42Hs. *EMBO J.* 15:2997–3005.

Jeong, H.W., Z. Li, M.D. Brown, and D.B. Sacks. 2007. IQGAP1 binds Rap1 and modulates its activity. *J. Biol. Chem.* 282:20752–20762. doi:10.1074/jbc.M700487200

Jin, A., T. Kurosu, K. Tsuji, D. Mizuchi, A. Arai, H. Fujita, M. Hattori, N. Minato, and O. Miura. 2006. BCR/ABL and IL-3 activate Rap1 to stimulate the B-Raf/MEK/Erk and Akt signaling pathways and to regulate proliferation, apoptosis, and adhesion. *Oncogene.* 25:4332–4340. doi:10.1038/sj.onc.1209459

Joyal, J.L., R.S. Annan, Y.D. Ho, M.E. Huddleston, S.A. Carr, M.J. Hart, and D.B. Sacks. 1997. Calmodulin modulates the interaction between IQGAP1 and Cdc42. Identification of IQGAP1 by nanoelectrospray tandem mass spectrometry. *J. Biol. Chem.* 272:15419–15425. doi:10.1074/jbc.272.24.15419

Kawasaki, H., G.M. Springett, S. Toki, J.J. Canales, P. Harlan, J.P. Blumenstiel, E.J. Chen, I.A. Bany, N. Mochizuki, A. Ashbacher, et al. 1998. A Rap guanine nucleotide exchange factor enriched highly in the basal ganglia. *Proc. Natl. Acad. Sci. USA.* 95:13278–13283. doi:10.1073/pnas.95.22.13278

Kurachi, H., Y. Wada, N. Tsukamoto, M. Maeda, H. Kubota, M. Hattori, K. Iwai, and N. Minato. 1997. Human SPA-1 gene product selectively expressed in lymphoid tissues is a specific GTPase-activating protein for Rap1 and Rap2. Segregate expression profiles from a rap1GAP gene product. *J. Biol. Chem.* 272:28081–28088. doi:10.1074/jbc.272.44.28081

Kuroda, S., M. Fukata, M. Nakagawa, K. Fujii, T. Nakamura, T. Ookubo, I. Izawa, T. Nagase, N. Nomura, H. Tani, et al. 1998. Role of IQGAP1, a target of the small GTPases Cdc42 and Rac1, in regulation of E-cadherin- mediated cell-cell adhesion. *Science.* 281:832–835. doi:10.1126/science.281.5378.832

Li, Z., S.H. Kim, J.M. Higgins, M.B. Brenner, and D.B. Sacks. 1999. IQGAP1 and calmodulin modulate E-cadherin function. *J. Biol. Chem.* 274:37885–37892. doi:10.1074/jbc.274.53.37885

Li, Y., J. Yan, P. De, H.C. Chang, A. Yamauchi, K.W. Christopherson II, N.C. Paranavitana, X. Peng, C. Kim, V. Munugalavadla, et al. 2007. Rap1a null mice have altered myeloid cell functions suggesting distinct roles for the closely related Rap1a and 1b proteins. *J. Immunol.* 179:8322–8331.

Lin, J., M.J. Miller, and A.S. Shaw. 2005. The c-SMAC: sorting it all out (or in). *J. Cell Biol.* 170:177–182. doi:10.1083/jcb.200503032

Lin, K.B., S.A. Freeman, S. Zabetian, H. Brugger, M. Weber, V. Lei, M. Dang-Lawson, K.W. Tse, R. Santamaria, F.D. Batista, and M.R. Gold. 2008. The rap GTPases regulate B cell morphology, immune-synapse formation, and signaling by particulate B cell receptor ligands. *Immunity.* 28:75–87. doi:10.1016/j.immuni.2007.11.019

Lutz, M.B., R.M. Suri, M. Niimi, A.L. Ogilvie, N.A. Kukutsch, S. Rössner, G. Schuler, and J.M. Austyn. 2000. Immature dendritic cells generated with low doses of GM-CSF in the absence of IL-4 are maturation resistant and prolong allograft survival in vivo. *Eur. J. Immunol.* 30:1813–1822. doi:10.1002/1521-4141(200007)30:7<1813::AID-IMMU1813>3.0.CO;2-8

Mace, E.M., S.J. Monkley, D.R. Critchley, and F. Takei. 2009. A dual role for talin in NK cell cytotoxicity: activation of LFA-1-mediated cell adhesion and polarization of NK cells. *J. Immunol.* 182:948–956.

Maillet, M., S.J. Robert, M. Cacquevel, M. Gastineau, D. Vivien, J. Bertoglio, J.L. Zugaza, R. Fischmeister, and F. Lezoualc'h. 2003. Crosstalk between Rap1 and Rac regulates secretion of sAPPalpha. *Nat. Cell Biol.* 5:633–639. doi:10.1038/ncb1007

Malarkannan, S., J. Regunathan, H. Chu, S. Kutlesa, Y. Chen, H. Zeng, R. Wen, and D. Wang. 2007. Bcl10 plays a divergent role in NK cell-mediated cytotoxicity and cytokine generation. *J. Immunol.* 179:3752–3762.

Mason, C.S., C.J. Springer, R.G. Cooper, G. Superti-Furga, C.J. Marshall, and R. Marais. 1999. Serine and tyrosine phosphorylations cooperate in Raf-1, but not B-Raf activation. *EMBO J.* 18:2137–2148. doi:10.1093/emboj/18.8.2137

Orange, J.S., K.E. Harris, M.M. Andzelm, M.M. Valter, R.S. Geha, and J.L. Strominger. 2003. The mature activating natural killer cell immunologic synapse is formed in distinct stages. *Proc. Natl. Acad. Sci. USA.* 100:14151–14156. doi:10.1073/pnas.1835830100

Pearce, A.C., J.I. Wilde, G.M. Doody, D. Best, O. Inoue, E. Vigorito, V.L. Tybulewicz, M. Turner, and S.P. Watson. 2002. Vav1, but not Vav2, contributes to platelet aggregation by CRP and thrombin, but neither is required for regulation of phospholipase C. *Blood.* 100:3561–3569. doi:10.1182/blood.V100.10.3561

Razidlo, G.L., R.L. Kortum, J.L. Haferbier, and R.E. Lewis. 2004. Phosphorylation regulates KSR1 stability, ERK activation, and cell proliferation. *J. Biol. Chem.* 279:47808–47814. doi:10.1074/jbc.M406395200

Regunathan, J., Y. Chen, S. Kutlesa, X. Dai, L. Bai, R. Wen, D. Wang, and S. Malarkannan. 2006. Differential and nonredundant roles of phospholipase Cgamma2 and phospholipase Cgamma1 in the terminal maturation of NK cells. *J. Immunol.* 177:5365–5376.

Ren, J.G., Z. Li, and D.B. Sacks. 2007. IQGAP1 modulates activation of B-Raf. *Proc. Natl. Acad. Sci. USA.* 104:10465–10469. doi:10.1073/pnas.0611308104

Romano, D., M. Pertuit, R. Rasolonjanahary, J.V. Barnier, K. Magalon, A. Enjalbert, and C. Gerard. 2006. Regulation of the RAP1/RAF-1/extracellularly regulated kinase-1/2 cascade and prolactin release by the phosphoinositide 3-kinase/AKT pathway in pituitary cells. *Endocrinology.* 147:6036–6045. doi:10.1210/en.2006-0325

Rousseau-Merck, M.F., V. Pizon, A. Tavitian, and R. Berger. 1990. Chromosome mapping of the human RAS-related RAP1A, RAP1B, and RAP2 genes to chromosomes 1p12---p13, 12q14, and 13q34, respectively. *Cytogenet. Cell Genet.* 53:2–4. doi:10.1159/000132883

Roy, M., Z. Li, and D.B. Sacks. 2004. IQGAP1 binds ERK2 and modulates its activity. *J. Biol. Chem.* 279:17329–17337. doi:10.1074/jbc.M308405200

Roy, M., Z. Li, and D.B. Sacks. 2005. IQGAP1 is a scaffold for mitogen-activated protein kinase signaling. *Mol. Cell. Biol.* 25:7940–7952. doi:10.1128/MCB.25.18.7940-7952.2005

Rubinfeld, B., S. Munemitsu, R. Clark, L. Conroy, K. Watt, W.J. Crosier, F. McCormick, and P. Polakis. 1991. Molecular cloning of a GTPase activating protein specific for the Krev-1 protein p21rap1. *Cell.* 65:1033–1042. doi:10.1016/0092-8674(91)90555-D

Sacks, D.B. 2006. The role of scaffold proteins in MEK/ERK signalling. *Biochem. Soc. Trans.* 34:833–836. doi:10.1042/BST0340833

Schwamborn, J.C., and A.W. Püschel. 2004. The sequential activity of the GTPases Rap1B and Cdc42 determines neuronal polarity. *Nat. Neurosci.* 7:923–929. doi:10.1038/nn1295

Stork, P.J., and T.J. Dillon. 2005. Multiple roles of Rap1 in hematopoietic cells: complementary versus antagonistic functions. *Blood.* 106:2952–2961. doi:10.1182/blood-2005-03-1062

Tran, N.H., X. Wu, and J.A. Frost. 2005. B-Raf and Raf-1 are regulated by distinct autoregulatory mechanisms. *J. Biol. Chem.* 280:16244–16253. doi:10.1074/jbc.M501185200

Watanabe, T., S. Wang, J. Noritake, K. Sato, M. Fukata, M. Takefuji, M. Nakagawa, N. Izumi, T. Akiyama, and K. Kaibuchi. 2004. Interaction with IQGAP1 links APC to Rac1, Cdc42, and actin filaments during cell polarization and migration. *Dev. Cell.* 7:871–883. doi:10.1016/j.devcel.2004.10.017

Watford, W.T., B.D. Hissong, J.H. Bream, Y. Kanno, L. Muul, and J.J. O'Shea. 2004. Signaling by IL-12 and IL-23 and the immunoregulatory roles of STAT4. *Immunol. Rev.* 202:139–156. doi:10.1111/j.0105-2896.2004.00211.x

Yamaoka-Tojo, M., T. Tojo, H.W. Kim, L. Hilenski, N.A. Patrushev, L. Zhang, T. Fukai, and M. Ushio-Fukai. 2006. IQGAP1 mediates VE-cadherin-based cell-cell contacts and VEGF signaling at adherence junctions linked to angiogenesis. *Arterioscler. Thromb. Vasc. Biol.* 26:1991–1997. doi:10.1161/01.ATV.0000231524.14873.e7

Yin, X.L., S. Chen, J. Yan, Y. Hu, and J.X. Gu. 2002. Identification of interaction between MEK2 and A-Raf-1. *Biochim. Biophys. Acta.* 1589:71–76. doi:10.1016/S0167-4889(01)00188-4